On Fokker-Planck Equations for Turbulent Reacting Flows. Part 1. Probability Density Function for Reynolds-Averaged Navier–Stokes Equations

STEFAN HEINZ
*Fachgebiet Strömungsmechanik, Technische Universität München, Boltzmannstr. 15,
D-85747 Garching, Germany; E-mail: heinz@flm.mw.tum.de*

Abstract. The accurate treatment of finite-rate chemistry is possible by the application of stochastic turbulence models which generalize Reynolds-averaged Navier–Stokes equations. Usually, one considers linear stochastic equations. In this way, fluctuations are generated by uncorrelated forces and relax with a frequency that is independent of the actual fluctuation. It has been proved that such linear equations are well appropriate to simulate near-equilibrium flows. However, the inapplicability or unfeasibility of other methods also results in a need for stochastic methods for more complex flow simulations. Their construction requires an extension of the simple mechanism of linear stochastic equations. Two ways to perform this are investigated here. The first way is the construction of a stochastic model for velocities where the relaxation frequency depends on the actual fluctuation. This is a requirement to involve relevant mixing variations due to large-scale flow structures. The stochastic model developed is applied to the simulation of convective boundary layer turbulence. Comparisons with the results of measurements provide evidence for its good performance and the advantages compared to existing methods. The second way presented here is the construction of scalar equations which involve memory effects regarding to both the stochastic forcing and relaxation of fluctuations. This allows to overcome shortcomings of existing stochastic methods. The model predictions are shown to be in excellent agreement with the results of the direct numerical simulation of scalar mixing in stationary, homogeneous and isotropic turbulence. The consideration of memory effects is found to be essential to simulate correctly the evolution of scalar fields within the first stage of mixing.

Key words: consistent turbulence models, convective boundary layer turbulence, micromixing model, probability density function, Reynolds-averaged Navier–Stokes equations.

1. Introduction

Many relevant turbulent flows with high Reynolds, Schmidt, or Damköhler numbers cannot be calculated by solving the basic equations, i.e., by direct numerical simulation (DNS). First of all, one is often interested in the knowledge of ensemble-averaged velocities and scalars (mass fractions of species and temperature). Therefore, one uses the basic equations to construct transport equations for these quantities, which results in Reynolds-averaged Navier–Stokes (RANS) methods. Such equations can be solved much more efficiently than the basic equations

but their range of applicability is limited [40]. Particularly, their use to reacting flow simulations is problematic because of the appearance of unknown mean reaction rates in the RANS equations for the transport of species. The modeling of these unknown terms requires knowledge about the probability density function (PDF) of scalars, which is usually found to be coupled to the velocity PDF. The calculation of such joint velocity-scalar PDFs via transport equations is the concern of PDF methods [1, 6, 14, 23, 35, 37, 40]. It is relevant to note that PDF methods generalize RANS methods because a PDF model implies RANS models for PDF moments of arbitrary order [38, 40].

Different ways were proposed (for instance, by Kerstein [28–30] or Valiño and Dopazo [47]) but the predominant way to develop PDF methods is the construction of PDF transport equations that have the structure of Fokker–Planck equations [12, 13, 37, 40, 45, 48]. The models expressed by these equations may also be written as stochastic differential equations that have the structure of Equations (3.1a–3.1c), see Section 3 [16, 37, 40, 41]. Previously, such stochastic equations were used mostly as linear equations. From the view point of statistical mechanics, the use of such linear stochastic equations is appropriate for the simulation of near-equilibrium processes [33, 50, 51]. Accordingly, linear stochastic equations were proved to be applicable to the simulation of (reacting) channel or pipe flows [40].

However, there is also a need to simulate more complex flows by means of PDF methods. This is the case if relevant industrial or environmental processes (processes in the chemical process industry or chemistry in the atmospheric boundary layer) have to be assessed: DNS simulations are too expensive for such applications, and RANS methods suffer from their inherent closure problems. The problem arises from the fact that such flows often involve non-equilibrium processes. Examples for such processes are given by binary mixing that is characteristic for non-premixed combustion problems, or the updrafts and downdrafts in the convective atmospheric boundary layer (see the detailed explanations given in Sections 5 and 6). The simulation of non-equilibrium processes by means of PDF methods requires nonlinear stochastic equations. The development of such equations will be considered here. It will be explained how non-equilibrium effects modify the simple, linear (production-relaxation) mechanism of near-equilibrium processes.

The investigation of this question is not only relevant regarding the simulation of complex flows by means of stochastic methods, but it also enables a better insight into the range of applicability of various computational methods. First, our developments reveal the range of applicability of linear stochastic equations. This is a non-trivial question, which will be pointed out in Sections 5.1 and 6.1. Second, our developments represent alternatives to existing PDF methods for non-equilibrium flows, which were constructed by assuming the knowledge of a solution to the PDF transport equation, see [12, 13, 34, 42, 43, 49] and the references therein. These works assume that the result of the PDF evolution (the limiting PDF) is known. In contrast to this, the approaches to be developed here predict (in general non-analytical) limiting PDFs. One may expect that such predictions offer

advantages. Apart from the problem that a limiting PDF is often unavailable, the limiting PDF has to be non-analytical in general due to changes in space and time, effects of sources and velocity-scalar interactions. Third, our developments are of interest regarding the comparison of PDF with filter density function (FDF) methods, which generalize large-eddy simulation (LES) methods (in analogy to the generalization of RANS by PDF methods, see [40]). The difference between PDF and FDF methods is given by the fact that only small-scale processes are modeled in FDF methods, whereas processes at all scales are modeled within the frame of PDF methods. Consequently, the computational requirements related to FDF methods are higher than those of PDF methods, but this disadvantage can be compensated through the applicability of simple, linear stochastic equations. A more detailed investigation of this question will be provided in a companion paper [22].

The paper is organized as follows. Basics related to PDF and RANS methods are reviewed briefly in Section 2 to prepare the following developments. The Fokker–Planck model for the transport of the joint velocity-scalar PDF will be presented in Section 3. This will be done in conjunction with the development of a concept to construct linear and nonlinear stochastic equations for velocities and scalars. The construction of linear stochastic models for velocities and scalars in this way is addressed in Section 4. This development is extended in Section 5 where a nonlinear velocity model is investigated. The second approach to construct nonlinear stochastic differential equations is presented in Section 6 with reference to the transport of scalars. The resulting new findings about the mechanisms of non-equilibrium effects and the range of applicability of different PDF methods will be discussed in Section 7.

2. PDF and RANS Methods

To introduce the notation and to prepare the developments made in the following sections, this section deals with basics about PDF and RANS methods. The basic equations are given in Section 2.1. They will be used in Section 2.2 to derive the corresponding RANS equations. The generalization of these equations through PDF methods will be described in Section 2.3.

2.1. THE BASIC EQUATIONS

We consider a mixture of perfect gases. The conservation equations for the instantaneous mass density $\rho(\mathbf{x}, t)$, velocities $\mathbf{U}(\mathbf{x}, t) = (U_1, U_2, U_3)$ and scalars (the mass fractions of N species and temperature) $\mathbf{\Phi}(\mathbf{x}, t) = (\Phi_1, \ldots, \Phi_{N+1})$ may be written [31]

$$\frac{\partial \rho}{\partial t} + U_i \frac{\partial \rho}{\partial x_i} = -\rho \frac{\partial U_i}{\partial x_i}, \tag{2.1a}$$

$$\frac{\partial U_j}{\partial t} + U_i \frac{\partial U_j}{\partial x_i} = A_j, \tag{2.1b}$$

$$\frac{\partial \Phi_\alpha}{\partial t} + U_i \frac{\partial \Phi_\alpha}{\partial x_i} = A_\alpha, \tag{2.1c}$$

where A_j and A_α are introduced. By assuming a Newtonian fluid, they are given by

$$A_j = \rho^{-1} \frac{\partial}{\partial x_i} \rho \nu \left[\frac{\partial U_i}{\partial x_j} + \frac{\partial U_j}{\partial x_i} - \frac{2}{3} \frac{\partial U_k}{\partial x_k} \delta_{ij} \right] - \rho^{-1} \frac{\partial p}{\partial x_j} + F_j, \tag{2.2a}$$

$$A_\alpha = \rho^{-1} \frac{\partial}{\partial x_i} \rho \nu_{(\alpha)} \frac{\partial \Phi_\alpha}{\partial x_i} + S_\alpha, \tag{2.2b}$$

Repeated indices imply summation with the exception of subscripts in parentheses. ν is the kinematic viscosity, p the pressure and F_j any external force (the acceleration due to gravity). For the mass fractions ($\alpha = 1, N$), $\nu_{(\alpha)} = \nu/\text{Sc}$ is the molecular diffusivity, where Sc denotes the Schmidt number. For the temperature ($\alpha = N + 1$), $\nu_{(N+1)} = \nu/\text{Pr}$ is the thermal diffusivity, where Pr denotes the Prandtl number. S_α denotes source terms which are assumed to be known. Equations (2.1a–2.1c) are closed via the thermal equation of state, $p = p(\rho, \Phi)$.

2.2. RANS METHODS

It is known that the direct numerical integration of Equations (2.1a–2.1c), which is referred to as DNS, is restricted to flows with low or moderate Reynolds, Schmidt and Damköhler numbers [40]. A way to simulate flows with higher values of these characteristic numbers is to apply equations for ensemble-averaged velocities **U** and scalars **Φ**. Regarding the treatment of variable-density flows, it is advantageous to introduce such quantities as density-weighted means. This is done by defining the averaged value of any function $Q(\mathbf{U}(\mathbf{x}, t), \mathbf{\Phi}(\mathbf{x}, t), t)$ of velocities and scalars by

$$\bar{Q} = \langle \rho \rangle^{-1} \langle \rho Q \rangle, \tag{2.3}$$

where the brackets refer to the ensemble average. Fluctuations of Q will be denoted by $Q'' = Q - \bar{Q}$. An exception is made for fluctuations of U_i, Φ_α, A_i and A_α that are used frequently. They will be written as small quantities,

$$u_i = U_i - \bar{U}_i, \quad \phi_\alpha = \Phi_\alpha - \bar{\Phi}_\alpha, \quad a_i = A_i - \bar{A}_i, \quad A_\alpha = A_\alpha - \bar{A}_\alpha. \tag{2.4}$$

By adopting these definitions, the averaging of Equations (2.1a–2.1c) leads to the following equations for ensemble-averaged velocities **U** and scalars **Φ**,

$$\frac{\partial \langle \rho \rangle}{\partial t} + \bar{U}_i \frac{\partial \langle \rho \rangle}{\partial x_i} = -\langle \rho \rangle \frac{\partial \bar{U}_i}{\partial x_i}, \tag{2.5a}$$

$$\frac{\partial \bar{U}_j}{\partial t} + \bar{U}_i \frac{\partial \bar{U}_j}{\partial x_i} + \langle \rho \rangle^{-1} \frac{\partial \langle \rho \rangle \overline{u_i u_j}}{\partial x_i} = \bar{A}_j, \tag{2.5b}$$

$$\frac{\partial \bar{\Phi}_\alpha}{\partial t} + \bar{U}_i \frac{\partial \bar{\Phi}_\alpha}{\partial x_i} + \langle \rho \rangle^{-1} \frac{\partial \langle \rho \rangle \overline{u_i \phi_\alpha}}{\partial x_i} = \bar{A}_\alpha. \tag{2.5c}$$

These equations are called RANS equations of first order. Their use for turbulent reacting flow simulations suffers from the problem to close these equations, i.e., to model the unknown Reynolds stresses $\overline{u_i u_j}$, turbulent scalar fluxes $\overline{u_i \phi_\alpha}$ and averaged accelerations $\bar{A}_j$, $\bar{A}_\alpha$ in terms of $\langle \rho \rangle$, $\bar{U}_j$ and $\bar{\Phi}_\alpha$. Approximations for the Reynolds stresses $\overline{u_i u_j}$ and turbulent scalar fluxes $\overline{u_i \phi_\alpha}$ can be found by considering their transport equations (A.1a–A.1b) given in Appendix A. The most serious problem related to the use of (2.5a–2.5c) is to provide a closure for $\bar{A}_\alpha$, which involves the calculation of mean chemical reaction rates $\bar{S}_\alpha$. With the exception of the limits of very slow or fast chemistry, a solution to this problem requires knowledge about the PDF of scalars. This PDF is usually found to be coupled to the velocity PDF so that the joint velocity-scalar PDF has to be calculated.

2.3. PDF METHODS

This joint velocity-scalar PDF will be defined as density-weighted mean of the instantaneous PDF,

$$F(\mathbf{v}, \boldsymbol{\theta}, \mathbf{x}, t) = \overline{\delta \left(\mathbf{U}(\mathbf{x}, t) - \mathbf{v} \right) \delta(\boldsymbol{\Phi}(\mathbf{x}, t) - \boldsymbol{\theta})}. \tag{2.6}$$

The knowledge of this function enables the calculation of the means of arbitrary functions of velocities and scalars. To see this, we write the average of any function Q as

$$\overline{Q(\mathbf{U}, \boldsymbol{\Phi}, \mathbf{x}, t)} = \int d\mathbf{v} \, d\boldsymbol{\theta} \, F \, Q(\mathbf{v}, \boldsymbol{\theta}, \mathbf{x}, t). \tag{2.7}$$

This relation may be proved by adopting definition (2.6) of F and using the shifting and normalization properties of the delta function. F integrates to unity, as may be seen by setting $Q = 1$.

The transport equation for the velocity-scalar PDF F can be derived from (2.1a–2.1c) by means of standard methods. It reads [16, 37, 40, 41]

$$\frac{\partial}{\partial t} \langle \rho \rangle F + \frac{\partial}{\partial x_i} \langle \rho \rangle v_i F = -\frac{\partial}{\partial v_i} \langle \rho \rangle \overline{A_i \mid \mathbf{v}, \boldsymbol{\theta}} \, F - \frac{\partial}{\partial \theta_\alpha} \langle \rho \rangle \overline{A_\alpha \mid \mathbf{v}, \boldsymbol{\theta}} \, F, \tag{2.8}$$

where the conditional accelerations on the right-hand side are defined through the relations

$$\overline{A_i \mid \mathbf{v}, \boldsymbol{\theta}} = F^{-1} \, \overline{A_i \delta \left(\mathbf{U} - \mathbf{v} \right) \delta \left(\boldsymbol{\Phi} - \boldsymbol{\theta} \right)},$$
$$\overline{A_\alpha \mid \mathbf{v}, \boldsymbol{\theta}} = F^{-1} \, \overline{A_\alpha \delta \left(\mathbf{U} - \mathbf{v} \right) \delta \left(\boldsymbol{\Phi} - \boldsymbol{\theta} \right)}. \tag{2.9}$$

Inserting (2.2a–2.2b) into (2.9) reveals that the conditional accelerations do not appear as known functions in velocities and scalars. This leads to the need for their modeling, which will be addressed in the following sections.

It is worth emphasizing that the PDF transport equation (2.8) generalizes RANS equations. By multiplying (2.8) with the corresponding variables and integration over the velocity-scalar space, one may derive transport equations for PDF moments of any order from Equation (2.8). Further, the use of (2.2b) in (2.9) reveals that the known instantaneous source rates appear in (2.8) so that there is no need for modeling the effects of chemical reactions in velocity-scalar PDF methods [37].

3. The Fokker–Planck Model

A stochastic model for the variables considered will be introduced in Section 3.1. As shown in Section 3.2, this model corresponds to assumptions about the conditional accelerations in the PDF transport equation (2.8). The use of these relationships for the determination of coefficients of the stochastic model is described in Section 3.3.

3.1. NONLINEAR STOCHASTIC MODEL

The modeling of the evolution of fluctuating macroscopic variables by a diffusion process [16, 40, 41] can be justified by means of statistical mechanics [17, 18, 33, 50, 51]. The extraction of the dynamics of macroscopic variables from underlying deterministic dynamics of (microscopic) quantities leads to equations that may be written in the following way [39]:

$$\frac{\mathrm{d}}{\mathrm{d}t} x_i^* = U_i^*, \tag{3.1a}$$

$$\frac{\mathrm{d}}{\mathrm{d}t} U_i^* = \Gamma_i[\mathbf{U}^*, \mathbf{\Phi}^*] + F_i + b_{ik} \frac{\mathrm{d}W_k}{\mathrm{d}t}, \tag{3.1b}$$

$$\frac{\mathrm{d}}{\mathrm{d}t} \Phi_\alpha^* = \Omega_\alpha[\mathbf{U}^*, \mathbf{\Phi}^*] + S_\alpha + c_{\alpha\beta} \frac{\mathrm{d}W_\beta}{\mathrm{d}t}. \tag{3.1c}$$

Equations (3.1a–3.1c) will be considered as Ito-stochastic differential equations [16, 41]. x_i^* and U_i^* (the star is used throughout the paper to refer to modeled fluctuating variables) will be seen as the ith components of the position and velocity of a particle, respectively. Φ_α^* represents a scalar α (mass fractions of species or temperature) transported by a particle. It is worth emphasizing that the term 'particle' does not imply the consideration of real particles. It refers to the Monte Carlo solution of the PDF transport equation where the stochastic variables are interpreted as properties of notional particles [40]. Γ_i, Ω_α, b_{ik} and $c_{\alpha\beta}$ are any unknown functions of $\mathbf{x}^*$, $\mathbf{U}^*$, $\mathbf{\Phi}^*$ and t. F_i and S_α represent known source terms. $\mathrm{d}W_i/\mathrm{d}t$ is a Gaussian process with vanishing mean values, $\langle \mathrm{d}W_i/\mathrm{d}t \rangle = 0$, and

uncorrelated values at different times, $\langle dW_i/dt(t) \cdot dW_j/dt'(t') \rangle = \delta_{ij}\delta(t - t')$. The symbol δ_{ij} is the Kronecker delta and $\delta(t - t')$ the delta function. dW_β/dt has the same properties as dW_i/dt. These two noise processes are considered to be uncorrelated.

3.2. CONSISTENCY CONSTRAINTS

The stochastic model (3.1a–3.1c) implies an equation for the joint PDF of velocities and scalars. This equation has to be consistent with the basic PDF transport equation (2.8), this means the model (3.1a–3.1c) has to determine the conditional accelerations in (2.8). As explained in Appendix B, the corresponding relations are given by

$$\overline{A_i \mid \mathbf{v}, \boldsymbol{\theta}} = \Gamma_i + F_i - \frac{1}{2F}\frac{\partial b_{ij}^2 F}{\partial v_j},$$

$$\overline{A_\alpha \mid \mathbf{v}, \boldsymbol{\theta}} = \Omega_\alpha + S_\alpha - \frac{1}{2F}\frac{\partial c_{\alpha\beta}^2 F}{\partial \theta_\beta}, \tag{3.2}$$

where $b_{ij}^2 = b_{ik}b_{jk}$ and $c_{\alpha\beta}^2 = c_{\alpha\mu}c_{\beta\mu}$. The equation that follows from the use of (3.2) in (2.8) is called a Fokker–Planck equation.

It is essential to emphasize that the Fokker–Planck model (3.2) does not solve the problem to derive a closed PDF transport equation. The latter requires the specification of the coefficients Γ_i, Ω_α, b_{ij} and $c_{\alpha\beta}$ as explicit functions in velocities and scalars. The modeling of b_{ij} can often be solved successfully by adopting the standard parametrization $b_{ik} = \sqrt{C_0\epsilon}\,\delta_{ik}$, where ϵ is the mean dissipation rate of turbulent kinetic energy and C_0 a constant [40]. An appropriate parametrization for $c_{\alpha\beta}$ will be derived in Section 6. The modeling of Γ_i and Ω_α is the remaining problem. A way for solving this question on the basis of the relations (3.2) will be described next.

3.3. THE DETERMINATION OF $\boldsymbol{\Gamma}$ AND $\boldsymbol{\Omega}$

First, we split (3.2) into relations for means and fluctuations of Γ_i and Ω_α. By multiplying (3.2) with F and integration, $\bar{\Gamma}_i$ and $\bar{\Omega}_\alpha$ are found to obey

$$\bar{A}_i = \bar{\Gamma}_i + \bar{F}_i, \quad \bar{A}_\alpha = \bar{\Omega}_\alpha + \bar{S}_\alpha. \tag{3.3}$$

These relations assure the consistency between the transport equations for mean velocities and scalars that are implied by the basic equations and the stochastic model, respectively. By adopting (3.3), the relations (3.2) can be rewritten into the following relations for Γ_i'' and Ω_α'':

$$\overline{a_i - F_i'' \mid \mathbf{v}, \boldsymbol{\theta}} = \Gamma_i'' - \frac{1}{2F}\frac{\partial b_{ij}^2 F}{\partial v_j},$$

$$\overline{a_\alpha - S_\alpha'' \mid \mathbf{v}, \boldsymbol{\theta}} = \Omega_\alpha'' - \frac{1}{2F}\frac{\partial c_{\alpha\beta}^2 F}{\partial \theta_\beta}. \tag{3.4}$$

Equations (3.4) can also be written as relations for all the moments of the conditional accelerations. To see this, we multiply (3.4) with FQ, where Q is any function of velocities or scalars. The resulting relations read

$$\overline{Q(a_i - F_i'')} = \overline{Q\Gamma_i''} + \frac{1}{2}\overline{\frac{\partial Q}{\partial v_j}b_{ij}^2}, \quad \overline{Q(a_\alpha - S_\alpha'')} = \overline{Q\Omega_\alpha''} + \frac{1}{2}\overline{\frac{\partial Q}{\partial \theta_\beta}c_{\alpha\beta}^2}, \quad (3.5)$$

where partial integration is used to obtain the last terms.

The relations (3.5) can be used in the following way to calculate Γ_i'' and Ω_α''. The first step is the specification of the order of the RANS model considered (for instance a second-, third- or fourth-order model). The notion about the varying influence of moments of higher than second-order corresponds to the concept to construct statistically most-likely (SML-) PDFs, see the explanations given in Appendix C. The second step is the extension of the RANS model considered to a corresponding PDF model. One may easily prove that the consideration of second-, third- or fourth-order RANS models implies the need to consider Γ_i'' and Ω_α'' as linear, quadratic or cubic functions of velocities and scalars, respectively. The last step is to specify Q in (3.5) so that unique relations between the coefficients of the linear, quadratic or cubic terms of Γ_i'' and Ω_α'' with turbulence statistics are obtained. These relations then permit the calculation of the coefficients of Γ_i'' and Ω_α''.

To illustrate this approach, let us assume that we have chosen only the means and variances of velocities and scalars to be the relevant variables. Correspondingly, we have to specify Γ_i and Ω_α as linear functions of velocities and scalars

$$\Gamma_i = \bar{\Gamma}_i + G_{im}(U_m^* - \bar{U}_m) + G_{i\mu}(\Phi_\mu^* - \bar{\Phi}_\mu),$$

$$\Omega_\alpha = \bar{\Omega}_\alpha + G_{\alpha\mu}(\Phi_\mu^* - \bar{\Phi}_\mu) + G_{\alpha m}(U_m^* - \bar{U}_m). \tag{3.6}$$

The physical relevance of considering these terms will be discussed in Section 4.1. We apply (3.6) in (3.5) and set $Q = u_j$ and $Q = \phi_\alpha$. This results in the following relations:

$$\overline{(a_i - F_i'')u_j} = G_{im}\overline{u_m u_j} + G_{i\mu}\overline{\phi_\mu u_j} + \frac{1}{2}\overline{b_{ij}^2},$$

$$\overline{(a_\alpha - S_\alpha'')\phi_\beta} = G_{\alpha m}\overline{u_m \phi_\beta} + G_{\alpha\mu}\overline{\phi_\mu \phi_\beta} + \frac{1}{2}\overline{c_{\alpha\beta}^2},$$

$$\overline{(a_i - F_i'')\phi_\alpha} = G_{im}\overline{u_m \phi_\alpha} + G_{i\mu}\overline{\phi_\mu \phi_\alpha},$$

$$\overline{(a_\alpha - S_\alpha'')u_i} = G_{\alpha m}\overline{u_m u_i} + G_{\alpha\mu}\overline{\phi_\mu u_i}. \tag{3.7}$$

For specified parametrizations of b_{ij}^2 and $c_{\alpha\beta}^2$, the relations (3.7) represent a unique relationship between a second-order RANS model and a linear stochastic model.

First, they provide the coefficients G_{im}, $G_{i\mu}$, $G_{\alpha\mu}$ and $G_{\alpha m}$ of the model (3.6) for specified acceleration correlations. Second, they provide the acceleration correlations on the left-hand sides for specified coefficients of the stochastic model. In correspondence to the properties of the relations (3.2), the relations (3.7) provide more constraints than found by the comparison of second-order RANS models that follow from Equation (2.8) and the stochastic model (3.1a–3.1c), respectively. The latter approach only leads to the sum of the expressions in the last line of (3.7), i.e., the coefficients of (3.6) cannot be specified completely [18]. Consequences for turbulence modeling that result from this difference to previous concepts will be pointed out in Section 4.

The relations (3.7) can be used in different ways to calculate the coefficients G_{im}, $G_{i\mu}$, $G_{\alpha\mu}$ and $G_{\alpha m}$ of the model (3.6). One way is to apply measurements of the acceleration correlations to obtain these coefficients. This will be demonstrated in Section 5. A second way is to parametrize the coefficients G_{im}, $G_{i\mu}$, $G_{\alpha\mu}$ and $G_{\alpha m}$, and to estimate then the open parameters by means of the acceleration correlations. This way will be pointed out in Section 4.

4. Linear Stochastic Modeling of Velocity and Scalar Fields

First, we demonstrate the implications of the method to determine $\boldsymbol{\Gamma}$ and $\boldsymbol{\Omega}$ for the construction of linear stochastic equations. This is relevant because most of the stochastic simulations of turbulent reacting flows are performed by means of linear equations. It is worth emphasizing that the following explanations differ from a previous analysis of Pope [38] by the consideration of velocity-scalar interactions and the use of the coefficient relations (3.7). The model considered will be introduced in Section 4.1, and the coefficient relations that result from the relations (3.7) are given in Section 4.2. Section 4.3 then deals with conclusions about the construction of linear stochastic models and second-order RANS models.

4.1. THE MODEL CONSIDERED

To derive concrete conclusions from the relations (3.7), we specify the expressions (3.6) for the coefficients of the stochastic model (3.1a–3.1c) in the following way:

$$\Gamma_i = \bar{\Gamma}_i - \left[\frac{c_1^*}{2\tau} \delta_{ik} - c_2^* \frac{\partial \bar{U}_i}{\partial x_k} \right] (U_k^* - \bar{U}_k) - c_3^* F_i'', \tag{4.1a}$$

$$\Omega_\alpha = \bar{\Omega}_\alpha - \frac{c_{\varphi 1}^*}{2\tau} (\Phi_\alpha^* - \bar{\Phi}_\alpha) + \frac{c_{\varphi 2}^*}{2\tau} \overline{\phi_\alpha u_i} \, V^{-1}{}_{ik} (U_k^* - \bar{U}_k). \tag{4.1b}$$

Relation (4.1a) assumes G_{ik} in (3.6) to be proportional to two frequencies: the shear $\partial \bar{U}_i / \partial x_k$, which determines the production of turbulence, and the inverse dissipation time scale of turbulence $\tau = k/\epsilon$, where $k = \overline{u_j u_j}/2$ is the turbulent kinetic energy. More general forms of G_{ik} (which can be seen to involve shear

of higher than first-order) may be considered [40]. However, their introduction results in the need for additional constraints, as pointed out below. Further, we specified $G_{i\mu}(\Phi^*_\mu - \bar{\Phi}_\mu) = -c^*_3 F''_i$, where F''_i may represent the influence of buoyancy on the velocity field [19, 21]. By adopting the Boussinesq approximation, F''_i is given by $F''_i = \beta g \delta_{i3}(T - \bar{T})$, where β is the thermal expansion exponent, g the acceleration due to gravity and T the temperature. x_3 is chosen to be the vertical coordinate. In (4.1b), the second term on the right-hand side appears in correspondence to the velocity term in (4.1a). The suitability of the specification of the coefficient of the velocity term (its physical effect is described in the second part of this paper [22, section 4.3]) will be shown below, see (4.3c). The effects of scalar gradients are involved in this way by the consideration of velocity-scalar correlations [15]. V^{-1} denotes the inverse velocity variance matrix, i.e., V has elements $V_{ij} = \overline{u_i u_j}$. The choice of the parameters c^*_1, c^*_2, c^*_3 and $c^*_{\varphi 1}$, $c^*_{\varphi 2}$ will be discussed below.

We complement (4.1a–4.1b) by adopting for the coefficient b_{ij} in (3.1b) the parametrization

$$b_{ij} = \sqrt{C_0 \epsilon} \delta_{ij}. \tag{4.2}$$

This expression assures that the Lagrangian velocity structure function which follows from (3.1b) is consistent with implications of Kolmogorov's theory [37, 40, 45]. The structure of $c_{\alpha\beta}$ in (3.1c) will be pointed out in Section 6. There is no need to specify $c_{\alpha\beta}$ for the following analysis.

4.2. COEFFICIENT RELATIONS

By adopting the expressions (4.1a–4.1b) and (4.2) for the coefficients of the stochastic model (3.1a–3.1c) in the relations (3.7), one finds the acceleration correlations in the variance equations (A.1a–A.1c) presented in Appendix A to be given by

$$\overline{(a_i - F''_i)u_j} = -\frac{c^*_4}{3}\epsilon\delta_{ij} - \frac{c^*_1}{2\tau}\left(\overline{u_i u_j} - \frac{2}{3}k\delta_{ij}\right)$$

$$+ c^*_2\left(\frac{\partial \bar{U}_i}{\partial x_k}\overline{u_k u_j} + \frac{P_S}{3}\delta_{ij}\right) - c^*_3\left(\overline{F''_i u_j} - \frac{P_B}{3}\delta_{ij}\right), \tag{4.3a}$$

$$\overline{(a_i - F''_i)\phi_\beta} = -\frac{c^*_1}{2\tau}\overline{u_i\phi_\beta} + c^*_2\frac{\partial \bar{U}_i}{\partial x_k}\overline{u_k\phi_\beta} - c^*_3\overline{F''_i\phi_\beta}. \tag{4.3b}$$

$$\overline{(a_\alpha - S''_\alpha)u_i} = \frac{c^*_{\varphi 2} - c^*_{\varphi 1}}{2\tau}\overline{\phi_\alpha u_i}, \tag{4.3c}$$

$$\overline{(a_\alpha - S''_\alpha)\phi_\beta} = -\frac{c^*_{\varphi 1}}{2\tau}\overline{\phi_\alpha\phi_\beta} + \frac{c^*_{\varphi 2}}{2\tau}\overline{\phi_\alpha u_k}V^{-1}{}_{ki}\overline{u_i\phi_\beta} + \frac{1}{2}\overline{c^2_{\alpha\beta}}, \tag{4.3d}$$

where the abbreviation c_4^* is given by the expression

$$c_4^* = c_1^* + c_2^* \frac{P_S}{\epsilon} + c_3^* \frac{P_B}{\epsilon} - \frac{3}{2} C_0, \tag{4.4}$$

and $P_S = -(\partial \bar{U}_m / \partial x_k) \overline{u_k u_m}$ and $P_B = \overline{F_k'' u_k}$ refer to the production due to shear and body forces, respectively, in the equation for the turbulent kinetic energy.

The comparison of (4.1a–4.1b) with (3.7) shows that the coefficients of (4.1a–4.1b) cannot be determined completely in terms of the acceleration correlations because G_{ik} involves two open parameters. Thus, an additional constraint is needed to calculate the parameter c_1^*. Such a constraint follows from Kolmogorov's theory [40], which implies $c_4^* = 1$. Hence, we obtain

$$c_1^* = 1 + \frac{3}{2} C_0 - c_2^* \frac{P_S}{\epsilon} - c_3^* \frac{P_B}{\epsilon}. \tag{4.5}$$

By adopting (4.5), we have for specified C_0 and $c_{\alpha\beta}$ a unique relationship between the stochastic model that applies (4.1a–4.1b) and the corresponding second-order RANS model: the right-hand sides of (4.3a–4.3d) determine the acceleration correlations, and the acceleration correlations can be used to calculate the parameters c_2^*, c_3^* and $c_{\varphi1}^*$, $c_{\varphi2}^*$ of the stochastic model. The stochastic and second-order RANS models obtained in this way will be compared to existing methods next.

4.3. IMPLICATIONS FOR THE CONSTRUCTION OF STOCHASTIC AND RANS MODELS

Regarding the construction of stochastic models, the difference to existing methods is given by the derivation of the expressions (4.3a–4.3d), which are a consequence of (3.2). Previously, the comparison of variance transport equations that follow from a stochastic model with corresponding equations that follow from averaging (and modeling) the basic equations resulted in the sum of the relations (4.3b–4.3c) [18]. In this way, no constraint for the parameter $c_{\varphi2}^*$ is obtained. In contrast to this, the derivation of (4.3c) permits its calculation. As a consequence of Kolmogorov's theory, we know that the left-hand side of Equation (4.3c) should vanish for high-Reynolds number flows. This implies $c_{\varphi2}^* = c_{\varphi1}^*$. The remaining parameters c_2^*, c_3^* and $c_{\varphi1}^*$ (c_1^* follows from (4.5) after specification of C_0) needed to close the stochastic model can be determined by measurements of the acceleration correlations on the left-hand sides of (4.3a–4.3b) and (4.3d), as demonstrated in Section 5. Experience obtained by RANS modeling provides support for the use of the values $c_2^* = c_3^* = 0.5$ (according to Launder [32] one applies $c_2^* = c_3^* = 0.6$ in (4.3a) and $c_2^* = c_3^* = 0.4$ in (4.3b)) and $c_{\varphi1}^* = 2.0$ [37, 40].

The stochastic model obtained in this way implies a second-order RANS model. The comparison of this model with usual second-order RANS models discussed by Launder [32] reveals the following differences. The effects of velocity-scalar correlations and $c_{\alpha\beta}$ are usually neglected in the scalar variance equation (A.1c)

given in Appendix A. Instead of the expression (4.5) found for c_1^* here, one usually assumes c_1^* to be constant. In the velocity variance equation (A.1a) one applies the value $c_1^* = 1.8$, whereas the value $c_1^* = 5.8$ [32] is used in the turbulent scalar flux equation (A.1b). Consequently, such second-order RANS models cannot be seen to represent consistent methods: one applies different models for the acceleration fluctuations a_i and a_α on the right-hand sides of (A.1a–A.1c). The relevance of such imbalances is known [10, 38].

5. Nonlinear Stochastic Modeling of Velocity Fields

The extension of linear stochastic equations for velocities to methods for non-equilibrium flow simulations will be addressed now. First, the problem of applying linear stochastic equations to such flows will be pointed out in Section 5.1. The linear stochastic theory considered in Section 4 will be extended to a cubic stochastic model in Section 5.2. Section 5.3 deals with a comparison of this model with methods applied previously to non-equilibrium flow simulations. The performance of the cubic model will be assessed in Section 5.4, where PDF simulations of convective boundary-layer (CBL) turbulence are compared to measurements.

5.1. THE LIMITATIONS OF THE APPLICABILITY OF LINEAR STOCHASTIC EQUATIONS

The question about the range of applicability of linear stochastic equations cannot be seen to be trivial. It is essential to note that their use is not restricted to flows with Gaussian PDFs. The consideration of spatial variations of the coefficients in stochastic equations implies spatial variance gradients which produce triple correlations (this may be seen in terms of the transport equations for second- and third-order moments). However, the deviations from Gaussian PDF shapes obtained in this way are too small to describe the non-Gaussian PDF shapes found in CBL turbulence, and it can be concluded that the use of linear stochastic equations in that situation has significant shortcomings [20]. The reason for this is that the bimodal structure of this flow is not simulated. The mixing frequency (the negative coefficient of the velocity term in (4.1a)) is considered to be independent of the actual value of the velocity so that the differences between the turbulent mixing of updrafts and downdrafts in the CBL are neglected.

The conclusion that linear stochastic equations are (in general) inapplicable to perform accurate simulations of flows that involve coherent structures is supported by previous applications of PDF and RANS methods to such flows. There exists broad evidence that nonlinear stochastic models are required to calculate the diffusion of species in the convective atmospheric boundary layer, see [34, 42, 43, 49] and the references therein. These models were constructed such that the second-, third- and fourth-order moments of the modeled velocity PDF agree with measurements. Particularly, information about third- and fourth-order moments

is used to characterize the bimodal PDF structure which cannot be reflected by restricting the consideration to means and variances. In accord with the explanations given above regarding the relations between stochastic and RANS models, this experience is confirmed by the application of RANS methods to such non-equilibrium flows. Second-order RANS methods (which correspond to the use of linear stochastic equations) are found to perform poorly in the prediction of even basic turbulent flows that are far from equilibrium [26, 44]. The consideration of transport equations for third- and fourth-order moments for such (convective or stratified) flow simulations was found to be a suitable way to improve significantly the performance of second-order RANS methods, see [2–5, 24, 27] and the references therein.

5.2. CUBIC STOCHASTIC MODEL

In accord with the explanations given in Section 5.1, we will construct a stochastic model as generalization of a fourth-order RANS model, this means a stochastic model that is capable of representing the transport of the first four PDF moments according to any fourth-order RANS model considered. As explained in Section 3, this requires the extension of expression (4.1a) for $\mathbf{\Gamma}$ to a cubic model. By restricting the consideration to velocity fields (scalar fields could be involved straightforwardly by extending the set of stochastic variables considered), this model for $\mathbf{\Gamma}$ reads

$$\Gamma_i = \bar{\Gamma}_i - G_{ikl} V_{kl} - G_{iklm}\overline{u_k u_l u_m} - M_{im}(U_m^* - \bar{U}_m). \tag{5.1}$$

$\bar{\Gamma}_i$ is determined by the first part of (3.3) combined with (2.5b). This way of writing the cubic model reveals the extension of linear stochastic methods through the consideration of a mixing frequency M_{im} that is a quadratic function of velocities,

$$M_{im} = -G_{im} - G_{ikm}(U_k^* - \bar{U}_k) - G_{iklm}(U_k^* - \bar{U}_k)(U_l^* - \bar{U}_l). \tag{5.2}$$

The second and third terms in (5.1) compensate the average of the last term. A model that applies (5.1) in (3.1b) will be referred to as cubic stochastic model below.

   The need to introduce M_{im} as a quadratic function of velocities becomes obvious by considering the relationships between the moment transport equations for second-, third- and fourth-order moments that follow from the stochastic model with the corresponding equations that follow from (2.8). By specifying the relations (3.5) appropriately, we find

$$\overline{(a_i - F_i'')u_j} = G_{ik} V_{kj} + G_{ikl}\overline{u_k u_l u_j} + G_{iklm}\overline{u_k u_l u_m u_j} + \frac{1}{2}\overline{b_{ij}^2}, \tag{5.3a}$$

$$\begin{aligned}
\overline{(a_i - F_i'')u_j u_n} &= G_{ik}\overline{u_k u_j u_n} + G_{ikl}[\overline{u_k u_l u_j u_n} - V_{kl} V_{jn}] \\
&\quad + G_{iklm}[\overline{u_k u_l u_m u_j u_n} - \overline{u_k u_l u_m}\, V_{jn}],
\end{aligned} \tag{5.3b}$$

$$\overline{(a_i - F_i'')u_j u_n u_m} = G_{ik}\overline{u_k u_j u_n u_m} + G_{ikl}[\overline{u_k u_l u_j u_n u_m} - V_{kl}\overline{u_j u_n u_m}]$$

$$+ G_{iklm'}[\overline{u_k u_l u_{m'} u_j u_n u_m} - \overline{u_k u_l u_{m'}}\,\overline{u_j u_n u_m}]$$

$$+ \frac{1}{2}(V_{nm}\overline{b_{ij}^2} + V_{jn}\overline{b_{im}^2} + V_{jm}\overline{b_{in}^2}). \qquad (5.3c)$$

For given b_{ij}, Equations (5.3a–5.3c) reveal a unique relationship between a fourth-order RANS model with the stochastic model that applies (5.1): the stochastic model provides the acceleration correlations that are needed to close a fourth-order RANS model, and, vice versa, the coefficients that appear in (5.1) can be determined for every choice of acceleration correlations. This relationship reveals the physical relevance of G_{ij}, G_{ijk} and G_{ijkl}: they provide information about the dynamics of second-, third- and fourth-order moments, respectively, in stochastic models.

5.3. COMPARISON WITH OTHER METHODS FOR NON-EQUILIBRIUM FLOWS

The cubic stochastic model agrees with methods applied previously to non-equilibrium flow simulations (see the references given in Section 5.1) by the fact that non-equilibrium effects are modeled by involving the dynamics of third- and fourth-order moments. However, there are also significant differences.

Nonlinear stochastic models that differ from the cubic model presented here can be obtained by means of the 'evolution-towards-a-limiting' (ETL-) PDF concept, see the explanations given in Appendix C. By comparing the cubic stochastic model with the corresponding fourth-order ETL-PDF model, we observe essential differences. First, due to changes in space and time and effects of external forces, buoyancy or chemical reactions, the limiting PDF resulting from the cubic model has a non-analytical form in general. Just these effects on the velocity field have to be neglected if any analytical PDF shape is assumed for the limiting PDF. Consequently, the cubic stochastic model is significantly more flexible than the fourth-order ETL-PDF model. The differences between these two types of stochastic models will be illustrated in Section 5.4.

In comparison to existing third- or fourth-order RANS models it is essential to note that the dynamics of third- or fourth-order moments were not considered previously (according to the author's knowledge) in acceleration models but only in conjunction with the treatment of turbulent transport. The need to consider such contributions results from the explanations given above. They simulate the influence of coherent (bimodal) structures on the dissipation in the variance transport equations, as may be seen in terms of equation (5.3a). Simple parametrizations of G_{ijk} and G_{ijkl} in (5.3a–5.3c) could be applied to improve the performance of closure models for such flows, but this is outside the scope of this paper.

5.4. APPLICATION TO CBL TURBULENCE SIMULATIONS

The cubic stochastic model could be applied to three-dimensional flow simulations but it will be useful in particular for computations of approximately one-dimensional (wall-bounded, buoyancy-driven, stratified boundary-layer) flows, which are clearly highly relevant [30]. An important example of such a flow is given by complex chemical processes (in reacting plumes) in the convective atmospheric boundary layer. The challenge related to the calculation of such flows is the simulation of the non-Gaussian velocity PDF, which has significant effects on the transport of reacting species [34]. Due to the fact that measured velocity PDF data are available for CBL turbulence, this flow was simulated to assess the performance of the cubic stochastic model. Previously, nonlinear stochastic models were developed for the convective atmospheric boundary-layer by adopting the ETL-PDF approach, see [34, 42, 43, 49] and the references therein. For reasons given in Appendix C, the performance of the cubic stochastic model will be compared to that of a fourth-order SML-PDF that serves as limiting PDF within the ETL-PDF approach. The use of a fourth-order SML-PDF was suggested by Du et al. [8, 9] as the most convenient way to simulate a flow by means of ETL-PDF models but this model was never compared to measurements.

According to (3.1a–3.1b) and (5.1), the stochastic model for the vertical velocity U_3^* may be written

$$\frac{\mathrm{d}}{\mathrm{d}t_*} x_{3*}^* = U_{3*}^*, \tag{5.4a}$$

$$\frac{\mathrm{d}}{\mathrm{d}t_*} U_{3*}^* = G_0 - G_2 \overline{u_{3*}^2} - G_3 \overline{u_{3*}^3} - M U_{3*}^* + b_{33} \frac{\mathrm{d}W}{\mathrm{d}t_*}, \tag{5.4b}$$

where the mixing frequency M is given by

$$M = -G_1 - G_2 U_{3*}^* - G_3 (U_{3*}^*)^2. \tag{5.5}$$

The lower star indicates that these quantities are made dimensionless by means of the convective velocity scale w_* and mixing layer height H,

$$t_* = \frac{t w_*}{H}, \quad x_{3*}^* = \frac{x_3^*}{H}, \quad U_{3*}^* = \frac{U_3^*}{w_*}, \quad \overline{u_{3*}^2} = \frac{\overline{u_3^2}}{w_*^2}, \quad \overline{u_{3*}^3} = \frac{\overline{u_3^3}}{w_*^3}. \tag{5.6}$$

The coefficients G_0, G_1, G_2 and G_3 were derived from the water tank data of Luhar et al. [34] on the basis of the first part of (3.3) and the relations (5.3a–5.3c). The mean acceleration and acceleration correlations were related to PDF moments by means of the moment transport equations (2.5b), (A.1a), (A.2) and (A.3). All the PDF moments required to calculate G_0, G_1, G_2 and G_3 were then derived from the measured PDF. The values obtained are given at the available vertical positions $0 \leq x_{3*} = x_3/H \leq 1$ in Table I. Analytical functions were obtained from these data by linear interpolation. These functions were applied in

Table I. The coefficients of the cubic stochastic model (5.4a–5.4b) as obtained from the water tank data of Luhar et al. [34].

x_{3*}	G_0	G_1	G_2	G_3	$\overline{u_{3*}^2}$	$\overline{u_{3*}^3}$
0.06	2.36	$0.78 - 1.08C_0$	$-3.12 + 0.31C_0$	$2.23 + 0.12C_0$	0.22	0.05
0.19	0.89	$0.80 - 0.52C_0$	$-1.01 + 0.47C_0$	$0.43 - 0.17C_0$	0.37	0.16
0.31	0.22	$0.18 - 0.40C_0$	$-0.20 + 0.49C_0$	$0.13 - 0.20C_0$	0.44	0.22
0.44	−0.15	$-0.20 - 0.44C_0$	$0.27 + 0.47C_0$	$0.04 - 0.17C_0$	0.43	0.22
0.56	−0.38	$-0.48 - 0.53C_0$	$0.42 + 0.45C_0$	$-0.03 - 0.13C_0$	0.40	0.22
0.69	−0.64	$-0.78 - 0.72C_0$	$0.43 + 0.38C_0$	$-0.15 - 0.05C_0$	0.33	0.16
0.81	−0.79	$-0.81 - 1.06C_0$	$0.27 + 0.25C_0$	$-0.25 + 0.13C_0$	0.24	0.09
0.94	−1.51	$-1.51 - 2.15C_0$	$-0.69 - 0.01C_0$	$-0.18 + 0.70C_0$	0.13	0.04

Equation (5.4b) by replacing x_{3*} through the actual particle position x_{3*}^*. For b_{33}, the usual parametrization

$$b_{33} = \sqrt{C_0 \epsilon_*} \qquad (5.7)$$

was applied, where the dimensionless dissipation rate of turbulent kinetic energy was taken as $\epsilon_* = 0.4$ [34]. C_0 is a constant which has to be estimated.

Boundary conditions were applied according to the analysis of Thomson and Montgomery [46]. A particle that would leave the computational domain due to its velocity was transported over a part of the time step until it reached the boundary. Then, the incident velocity v_i at the boundary was replaced by the reflected velocity v_r, which satisfies the equation

$$0 = \int_{v_r}^{\infty} dv_{3*}\, F_{3*} \cdot v_{3*} + \int_{-\infty}^{v_i} dv_{3*}\, F_{3*} \cdot v_{3*}. \qquad (5.8)$$

Here, $v_{3*} = v_3/w_*$ is the vertical sample space velocity and $F_{3*} = \overline{\delta(u_{3*} - v_{3*})}$ its PDF. All the details about this equation, which assures the correct PDF at the boundaries, can be found elsewhere [46]. The relationship between the incident and reflected velocity is shown in Figure 1, where the measured vertical velocity PDF was applied in (5.8). After replacing the particle velocity, the particle was transported over the remaining part of the time step with the new velocity.

Equations (5.4a–5.4b) were solved numerically in conjunction with boundary conditions according to (5.8). This was done by applying 5×10^5 particles and a time step $dt_* = 0.003$. According to the measurements, the PDF was obtained by means of the particles which were found within eight intervals in the x_{3*}-domain. For each of these x_{3*}-intervals, intervals $dv_{3*} = 0.1$ were applied to calculate the value of F_{3*} at v_{3*}. The lower and upper boundaries were taken at $x_{3*} = 1/16$ and $x_{3*} = 15/16$, respectively.
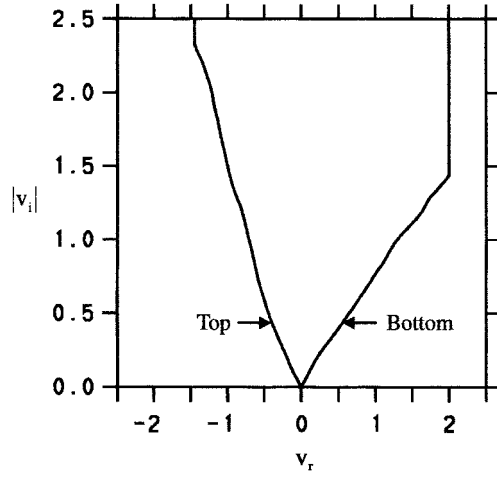
Figure 1. The reflected velocity v_r in dependence on the incident velocity v_i at the lower and upper boundaries according to Equation (5.8).
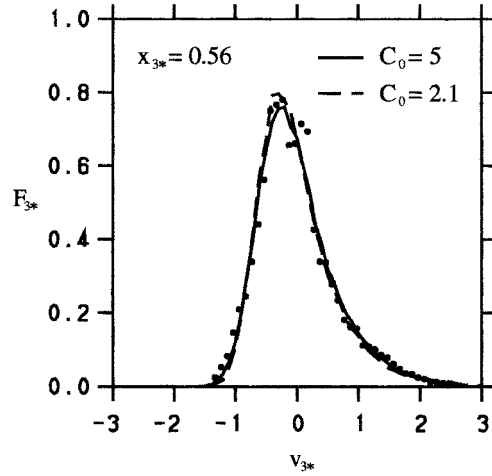

Figure 2. The predictions of the cubic stochastic model for the PDF F_{3*} of normalized vertical velocities v_{3*} at $x_{3*} = 0.56$ for different values of C_0. The results of the water tank experiments [33] are given as dots.

The calculation of C_0 requires a closer look at the mixing frequency, which may be written as

$$M = -G_1 \left\{ \left(1 + \frac{G_2}{2G_1} U_{3*}^* \right)^2 + [4G_1 G_3 - G_2^2] \left(\frac{U_{3*}^*}{2G_1} \right)^2 \right\}. \tag{5.9}$$

We have to demand that M is positive so that velocity fluctuations relax. The coefficient G_1 is negative provided $C_0 \geq 1.54$ (see Table I). Then, $M \geq 0$ when $4G_1 G_3 - G_2^2 \geq 0$. One may prove by means of the data given in Table I that the lat-

ter constraint is satisfied for the bulk of the CBL ($0.19 \leq x_{3*} \leq 0.69$) provided that $C_0 \geq 3$. For values $C_0 > 3$, we have inside the bracket of (5.9) two independent, positive contributions which cannot vanish simultaneously. Therefore, $M > 0$ in this case. The choice $C_0 = 3$ implies that the last term of (5.9) is small for the bulk of the CBL. The minimum of M is then zero, which is a plausible assumption. Thus, this consideration suggests the choice $C_0 = 3$. Its suitability is confirmed by Figure 2, where the effects of C_0 variations on the PDF shape are shown. We note that the choice $C_0 = 3$ agrees with the finding $C_0 = 3\pm0.5$ of Du et al. [9].

The stationary predictions of the cubic stochastic model and fourth-order SML-PDF model are compared to the results of the water tank measurements of Luhar et al. [34] in Figure 3. As may be seen, there is a good agreement between the calculated PDFs and the measurements. In particular, the typical skewness of the velocity PDF is well represented. Its appearance is explained in terms of the cubic stochastic model through a significant difference of the mixing intensity for negative and positive velocities. M is given in the middle of the CBL approximately by $M = 1.8(1 - 0.5U_{3*}^*)^2$. By considering the case $|U_{3*}^*| = 1$, we find that $M_- = 9M_+$, where M_- and M_+ denote M for $U_{3*}^* = -1$ and $U_{3*}^* = 1$, respectively. All the modeled PDFs underpredict somewhat the probability of very small velocities in the upper CBL, see Figure 3f. The predictions of the fourth-order SML-PDF model agree, basically, with those obtained previously by means of a superposition of two Gaussian PDFs [34]. This is of interest because there is one fitting parameter more available in the latter model, and confirms the reasoning for the choice of the limiting PDF as a SML-PDF. As expected, the performance of the cubic stochastic model is somewhat better than that of the fourth-order SML-PDF model with the exception of the PDF at $x_{3*} = 0.19$ where the coefficients change strongly (see Table I).

6. Nonlinear Stochastic Modeling of Scalar Fields

The extension of linear stochastic equations for scalars to methods for non-equilibrium flow simulations will be considered next. The range of applicability of linear equations will be pointed out in Section 6.1. A more general approach will be developed in Sections 6.2, 6.3 and 6.4. The performance of this scalar transport model will be assessed in Section 6.5 by comparing its predictions with the results of DNS.

6.1. THE LIMITATIONS OF THE APPLICABILITY OF LINEAR STOCHASTIC EQUATIONS

The model that is used in general to perform scalar mixing simulations is the 'interaction by exchange with the mean' (IEM) model. It is given by neglecting the stochastic term in (3.1c) and modeling Ω_α according to (4.1b) but without the velocity term. The problem related to this model is that the influence of noise on
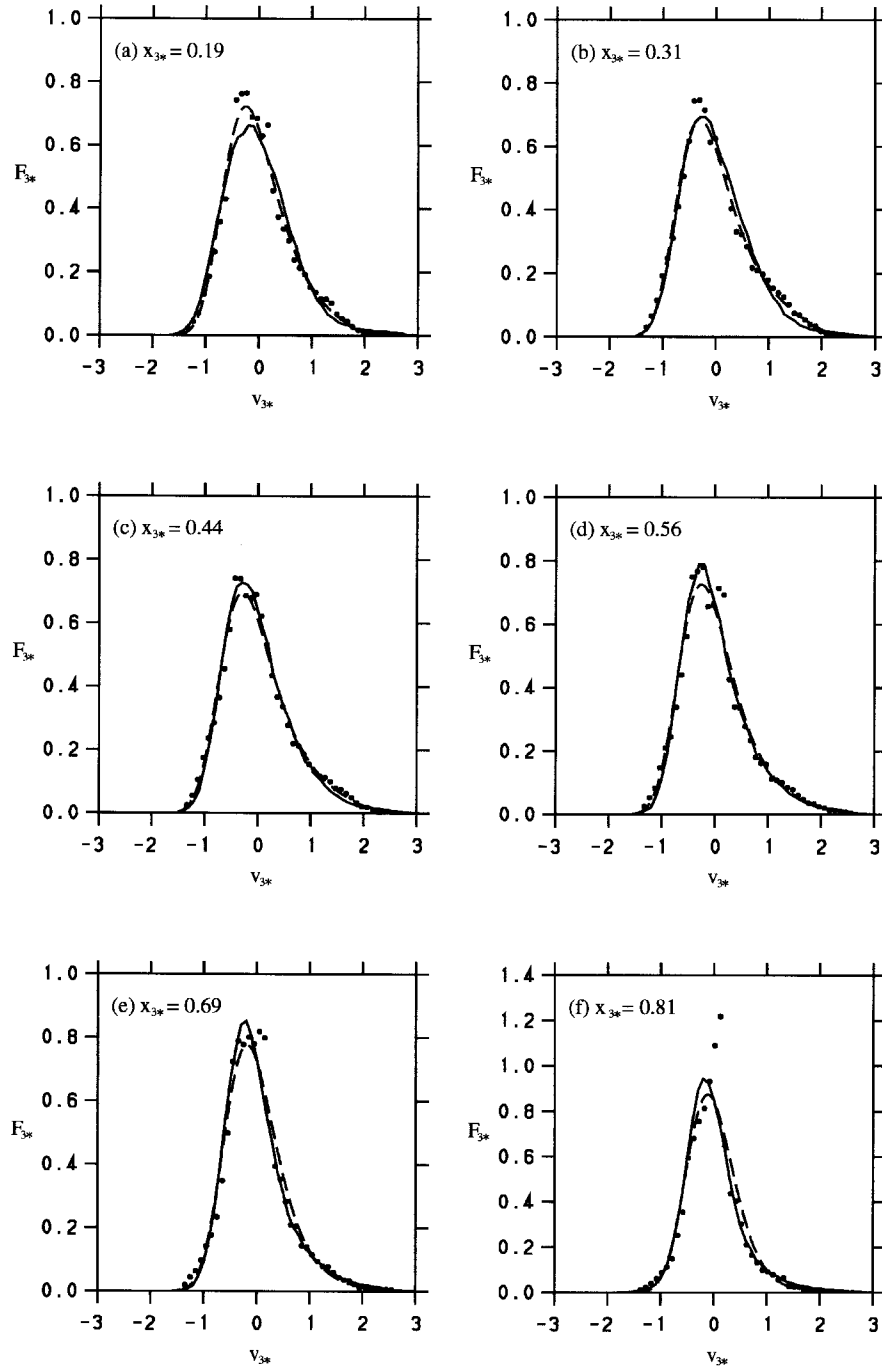
Figure 3. The same comparison as in Figure 2 for different heights x_{3*}, where $C_0 = 3$ was applied. The dashed line gives the prediction of the fourth-order SML-PDF model.

the scalar evolution is not considered. Many relevant non-premixed combustion problems are characterized by the appearance of strongly non-Gaussian (bimodal) initial PDFs, which evolve towards an equilibrium (Gaussian) PDF. This transition cannot be described in terms of the IEM model. The lack of noise generation implies that information about the initial state is never lost: the asymptotic PDF has the same shape as the initial PDF. In particular, one can show that the standardized scalar PDF (the PDF of scalars that are normalized to their variance) predicted by the IEM model never changes [37], see the discussion that follows Equation (6.10).

The consideration of a stochastic noise term that is independent of the actual scalar value is in general not an appropriate way to overcome this problem [12, 47]. Scalars have the characteristic property to be bounded: the convex region in sample space occupied by the scalars decreases with time [40]. This property cannot be satisfied if such a noise term is applied because there is a non-zero probability for the appearance of unphysical scalar values outside of bounds.

To describe both the loss of information about the initial state and the boundedness of scalars one needs a stochastic forcing in scalar equations that depends on the scalar – the noise term has to vanish for scalar values near bounds. The consideration of such noise processes has significant consequences. In general, scalars are found to be correlated over finite times (for example due to transport within one eddy). Thus, stochastic forces that involve scalars have to be correlated over finite times, too. Consequently, the scalar dynamics have to be described by a more general approach than used in Section 4. A methodology to obtain such generalized stochastic equations is the projection operator technique. It enables the extraction of the dynamics of relevant variables from underlying deterministic dynamics of (microscopic) quantities [17, 33, 50, 51]. In agreement with the requirements described above, the dynamics of variables considered are found to be driven by correlated stochastic forces.

6.2. GENERALIZED STOCHASTIC EQUATIONS

The application of the projection operator technique to the problem considered will be described now. To keep the development simple, we restrict the attention to the transport of a passive, inert scalar in statistically homogeneous velocity and scalar fields. In this case, the projection operator technique provides equations for the transport of a scalar Φ^*, which may be written in the following way [18]:

$$\frac{d\Phi^*}{dt} = \Psi^*, \tag{6.1a}$$

$$\frac{d\Psi^*}{dt} = -A\Psi^* - B\Phi^* + C\frac{dW}{dt}. \tag{6.1b}$$

Ψ^* refers to the scalar derivative that is defined through (6.1a). A, B and C are any deterministic functions of Φ^*, Ψ^* and time t. dW/dt denotes one component

of dW_i/dt which was defined in Section 3.1. The averages $\bar{\Phi}$ and $\bar{\Psi}$ have to be constant for the flow considered. For simplicity, they are set equal to zero.

To explain the physics of (6.1a–6.1b), it is advantageous to rewrite these equations into a standardized form. For that, we define a characteristic scalar variance decay time scale τ_φ in terms of the scalar variance,

$$\frac{1}{\tau_\varphi} = -\frac{1}{2\overline{\phi^2}}\frac{d\overline{\phi^2}}{dt}, \tag{6.2}$$

where ϕ denotes the scalar fluctuation as before. The introduction of τ_φ enables the definition of a dimensionless time scale $T = 2\int_0^t ds\,\tau_\varphi^{-1}$. Equation (6.2) then provides $\overline{\phi^2} = \overline{\phi^2(0)}\exp(-T)$. By adopting this expression, we can rewrite Equations (6.1a–6.1b) in terms of the standardized variables $\hat{\phi} = \Phi^*/\overline{\phi^2}^{1/2}$ and $\hat{\psi} = 0.5\hat{\phi} + 0.5\tau_\varphi\Psi^*/\overline{\phi^2}^{1/2}$,

$$\frac{d\hat{\phi}}{dT} = \hat{\psi}, \tag{6.3a}$$

$$\frac{d\hat{\psi}}{dT} = a\left\{-\hat{\psi} - b\hat{\phi} + c\frac{dW}{dT}\right\}. \tag{6.3b}$$

In (6.3b), we introduced the coefficients $a = (\tau_\varphi A - d\tau_\varphi/dt)/2 - 1$, $b = (\tau_\varphi^2 B - 2A + 1)/(4a)$ and $c = C\tau_\varphi^{1/2}/(2a^2\overline{\phi^2})^{1/2}$.

According to the concept presented in Section 3, we consider the transport equations for the variances of $\hat{\phi}$ and $\hat{\psi}$ in order to derive constraints for the coefficients a and b. These variance equations can be obtained by adopting the PDF transport equation that corresponds to the stochastic equations (6.3a–6.3b). The applied normalization implies that $\overline{\hat{\phi}^2} = 1$. The transport equation for $\overline{\hat{\phi}^2}$ then leads to $\overline{\hat{\phi}\hat{\psi}} = 0$, and the transport equation for $\overline{\hat{\phi}\hat{\psi}}$ implies the consistency constraint

$$b = a^{-1}\overline{\hat{\psi}^2}, \tag{6.4}$$

which determines the coefficient b. The transport equation for $\overline{\hat{\psi}^2}$ reads

$$\frac{d\overline{\hat{\psi}^2}}{dT} = -2a\,\overline{\hat{\psi}^2} + a^2\overline{c^2}. \tag{6.5}$$

One could try to use this relation for the estimation of the coefficient a. However, this is complicated because of the non-trivial structure of c and the fact that statistics of the standardized scalar derivative $\hat{\psi}$ is difficult to obtain. Therefore, we consider the coefficient a as a constant fitting parameter here, which is advantageous with reference to applications of the scalar model.

6.3. THE SCALAR DYNAMICS

The consideration of the model (6.1a–6.1b) in its standardized form (6.3a–6.3b) simplifies the explanation of the physics described in this way. For doing this, we will rewrite (6.3a–6.3b) into one equation for the scalar $\hat{\phi}$. First, we solve (6.3b) formally, which results in

$$\hat{\psi} = -\int_0^T dT' \exp\{-a(T - T')\}\overline{\hat{\psi}^2}(T')\hat{\phi}(T') + f(T), \tag{6.6a}$$

$$f(T) = a\int_0^T dT' \exp\{-a(T - T')\}c(T')\frac{dW}{dT'}(T'). \tag{6.6b}$$

To obtain (6.6a), we applied $\hat{\psi}(0) = 0$ which assures that $\overline{\hat{\phi}\hat{\psi}} = 0$. Further, we used $b = \overline{\hat{\psi}^2}/a$ to replace b, and we introduced the abbreviation $f(T)$ that is given through (6.6b). The function $f(T)$ vanishes in the mean, and its correlation function is given according to (6.6b) by

$$\overline{f(T)f(T')} = \overline{\hat{\psi}^2}(T')\exp\{-a(T - T')\}, \tag{6.7}$$

where $T \geq T'$ is assumed. The consistency of (6.7) at $T = T'$ can be seen by proving that $\overline{f^2}(T')$ satisfies the same transport equation as $\overline{\hat{\psi}^2}(T')$. Therefore, these two functions must be equal because $\overline{\hat{\psi}^2}$ vanishes initially as $\overline{f^2}(T')$. The use of (6.6a) combined with (6.7) in (6.3a) then results in the following form of the model (6.3a–6.3b):

$$\frac{d\hat{\phi}}{dT} = -\int_0^T dT' \overline{f(T)f(T')}\,\hat{\phi}(T') + f(T), \tag{6.8a}$$

$$\frac{df}{dT} = -a\,f + ac\frac{dW}{dT}, \tag{6.8b}$$

where (6.6b) is used to obtain Equation (6.8b). To be consistent with (6.6b), we have to demand that $f(0) = 0$.

We observe that the scalar equation (6.8a) is fully determined through the properties of the stochastic force f. This force simulates stochastic motions that appear randomly and disappear with a characteristic time scale a^{-1}. The generation and decay of these stochastic motions are modeled through the right-hand side of Equation (6.8b). In agreement with the requirements pointed out in Section 6.1, the scalar dynamics are found to be driven by correlated stochastic forces. The consideration of such memory effects regarding the forcing has to be complemented by

their incorporation into the relaxation term (the first term on the right-hand side of (6.8a)).

It is worth noting that the model (6.8a-b) reduces asymptotically to an extension of the often applied IEM model. In the limit of a vanishing correlation time $a^{-1} \to 0$, the force f becomes delta-correlated,

$$\overline{f(T)f(T')} = \frac{2}{a}\overline{\hat{\psi}^2}(T')\,\delta(T-T') = \overline{c^2}(T)\,\delta(T-T'). \tag{6.9}$$

The last expression is found by adopting the relation (6.5) in the limit $a^{-1} \to 0$, which is equivalent to neglecting the derivative on the left-hand side. The use of (6.9) in (6.8a) then results in

$$\frac{d\hat{\phi}}{dT} = -\frac{\overline{c^2}}{2}\hat{\phi} + c\frac{dW}{dT}. \tag{6.10}$$

This model generalizes the IEM model, which follows by setting $c = 0$. In this case, information about structures of the initial scalar PDF will not disappear in time, which is the well-known drawback of the IEM model [37, 40].

6.4. THE MODELING OF c

An important property of scalars is their characteristic boundedness [37, 40], which has implications for the modeling of c in (6.3b): the application of a coefficient c that is independent of the actual scalar value results in the appearance of unphysical scalar values outside of bounds. The boundedness constraint could be satisfied within the frame of Fokker–Planck equations by adopting boundary conditions [12, 13, 16, 41]. A way to tackle this problem is the application of the concept described in Section 5.4 with reference to the simulation of a convective boundary layer: by considering $\hat{\phi}$ as the position of a particle in scalar space and $\hat{\psi}$ as its velocity, the equations presented above could be applied. However, this requires information about the $\hat{\psi}$-PDF at the boundaries which is hardly available for complicated scalar fields. Thus, the solution of the boundedness problem through the use of boundary conditions cannot be considered to be appropriate in general. The suitability of simulating the flows considered by Juneja and Pope [25] in conjunction with reflection conditions at boundaries [12, 13] was investigated in preparation of the calculations described in Section 6.5. It was found that the significant overprediction of the PDF structure decay in the outer parts of the scalar PDF, which is observed if boundary conditions are not applied, can be limited in this way but this leads to the appearance of unphysical peaks of the PDFs at the boundaries.

Another way to guarantee the boundedness of scalar values consists in an appropriate specification of the coefficient c. This will be done here by assuming that c is non-zero only inside the lower and upper bounds of the scalar space $\hat{\phi}_-$ and $\hat{\phi}_+$, respectively, and given by the relation

$$c^2 = C_{\varphi 0}^*[(\hat{\phi} - \hat{\phi}_-)(\hat{\phi}_+ - \hat{\phi})]^n. \tag{6.11}$$

$C_{\varphi 0}^{*}$ is a proportionality factor that will be calculated in Section 6.5. The power n can be determined by the following arguments. One may easily check that the maximum of c^2 is given by

$$c_{\max}^2 = C_{\varphi 0}^{*} \left[\frac{\hat{\phi}_+ - \hat{\phi}_-}{2} \right]^{2n}. \tag{6.12}$$

The asymptotic model (6.10) reveals that $\overline{c^2}$ represents a characteristic frequency of the scalar relaxation. One has to expect this frequency $\overline{c^2}$ as the sum of independent contributions related to the lower and upper bounds. This implies $n = 0.5$ so that

$$c^2 = C_{\varphi 0}^{*} \sqrt{(\hat{\phi} - \hat{\phi}_-)(\hat{\phi}_+ - \hat{\phi})}. \tag{6.13}$$

The remaining question is the modeling of the evolution of the bounds $\hat{\phi}_-$ and $\hat{\phi}_+$. These functions have to satisfy deterministic equations, which should be linear in $\hat{\phi}_-$ and $\hat{\phi}_+$ according to the linear deterministic contributions in (6.3a–6.3b). Hence, we postulate

$$\frac{d}{dT} \hat{\phi}_\pm = \lambda \hat{\phi}_\pm, \tag{6.14}$$

where λ is a constant that has to be determined. The integration of (6.14) provides

$$\hat{\phi}_\pm(T) = \hat{\phi}_\pm(0) \exp(\lambda T). \tag{6.15}$$

The model (6.3a–6.3b) in conjunction with $b = \overline{\hat{\psi}^2}/a$, (6.13) and (6.15) will be referred to below as 'refined interaction by exchange with the mean' (RIEM) model. It guarantees the boundedness of scalars statistically: some scalar values may be found outside the bounds but the probability for such events is very small. This will be demonstrated by comparisons with DNS data in Section 6.5.

6.5. COMPARISON WITH DNS

The RIEM model will be tested by the comparison with the R92A-DNS data of scalar mixing in stationary, homogeneous and isotropic turbulence obtained by Juneja and Pope [25]. The Taylor-scale Reynolds number is $\mathrm{Re}_\lambda = 92$ in this simulation. Two initial PDFs $f_\varphi(\theta, t) = \overline{\delta(\phi(t) - \theta)}$ were considered close to $f_\varphi = [\delta(\theta - \sqrt{3}/2) + \delta(\theta + \sqrt{3}/2) + \delta(\theta)]/3$ (scalar 1) and $f_\varphi = [\delta(\theta - 1) + 2\delta(\theta + 0.5)]/3$ (scalar 2). It is worth emphasizing that the prediction of the evolution of these scalar fields is remarkably more challenging than previous comparisons with the DNS data of Eswaran and Pope [11]: the symmetric scalar-1 PDF contains modes which decay differently, and the scalar-2 PDF is strongly asymmetric.

The PDF evolution was considered in terms of the normalized scalar variance Φ_T defined by $\Phi_T^2 = \overline{\phi^2(T)}/\overline{\phi^2(0)} = e^{-T}$. This quantity is bounded, $0 \le \Phi_T \le 1$.
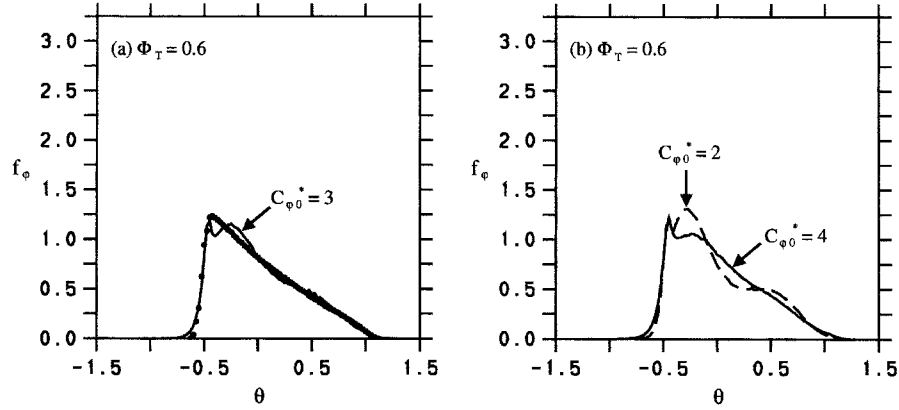
Figure 4. The RIEM model prediction (line) with $C_{\varphi 0}^* = 3$ is compared to Juneja and Pope's [25] DNS data of the scalar-2 PDF (dots) at $\Phi_T = 0.6$ in (a). The effect of $C_{\varphi 0}^*$-variations is shown in (b).

The initial values for $\hat{\phi}$ were chosen according to the DNS data for $\Phi_T = 1$. The $\hat{\psi}$-values were set equal to zero initially to satisfy the condition $\overline{\hat{\phi}\hat{\psi}} = 0$. Equations (6.3a–6.3b) were solved numerically by adopting 5×10^5 particles and a time step $dT = 0.002$. At the corresponding Φ_T, $f_\varphi(\theta)$ was calculated where intervals $\Delta\theta = 0.025$ were applied to calculate the value of f_φ at θ. The parameters of the bound model (6.15) were found by means of the DNS-data as $\lambda = 0.3$, $\hat{\phi}_-(0) = -1.90$ and $\hat{\phi}_+(0) = 1.90$ (scalar 1), $\hat{\phi}_-(0) = -0.93$ and $\hat{\phi}_+(0) = 2.08$ (scalar 2). The parameters a and $C_{\varphi 0}^*$ were fitted to achieve the best agreement with the DNS data. The value $a = 1$ was found as an optimal value. Figure 4a demonstrates the good performance of PDF simulations where $C_{\varphi 0}^* = 3$ was used. The effect of $C_{\varphi 0}^*$-variations is shown in Figure 4b. Only the scalar-2 DNS data were used to determine the model parameters. Hence, the assessment of PDF calculations of the scalar-1 evolution can be performed with independent data.

Figures 5a1, 5a2, 5b1, 5b2 and 6a1, 6a2, 6b1, 6b2 show that the results of these PDF simulations agree well with the corresponding DNS data. The most difficult task is the simulation of the non-equilibrium processes within the first stage of mixing, $0.7 \leq \Phi_T \leq 1$. The results of the PDF simulations are very similar as the DNS data, there are only minor differences. The mixing processes may be seen to be in the near-equilibrium stage for $\Phi_T \leq 0.6$, where T becomes greater than $a^{-1} = 1$. Here, the RIEM model predicts approximately the same PDF as found by DNS. The relevance of memory effects can be assessed through a comparison with the performance of the asymptotic model (6.10) combined with a constant c. For the latter, one finds an optimal value $c = 0.65$, which provides the best agreement between the model prediction and the scalar-2 DNS data at $\Phi_T = 0.6$. The resulting scalar PDF calculations are shown in Figures 5c1, 5c2 and 6c1, 6c2. These figures reveal significant deviations between the predictions of the RIEM and asymptotic
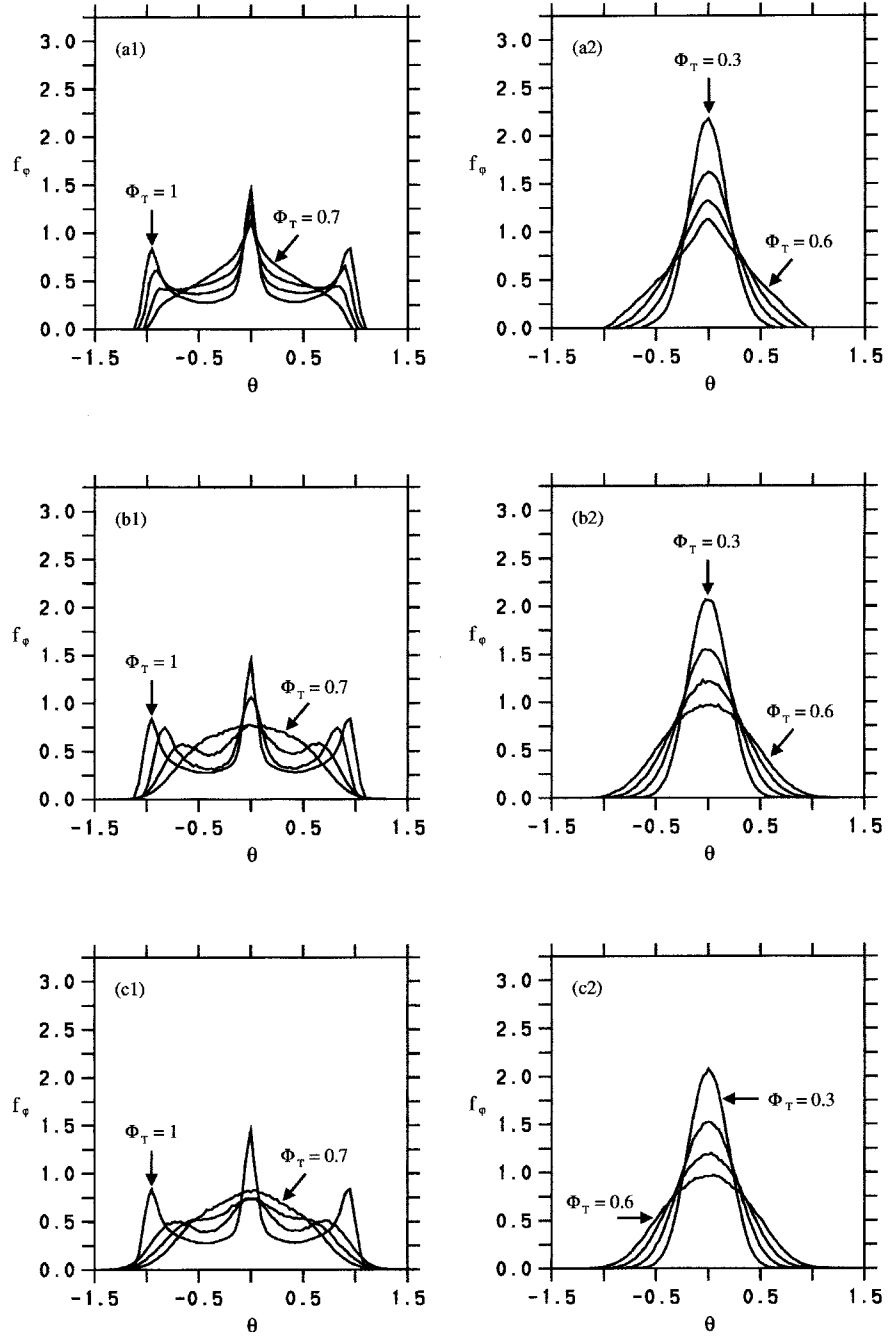
Figure 5. The scalar-1 PDF evolution in stationary, homogeneous and isotropic turbulence is given in (a1) and (a2) according to the DNS data of Juneja and Pope [25]. The corresponding predictions of the RIEM model are shown in (b1) and (b2), where $C_{\varphi 0}^* = 3$ is applied. Figures (c1) and (c2) show the predictions of the asymptotic model (6.10) combined with $c = 0.65$.
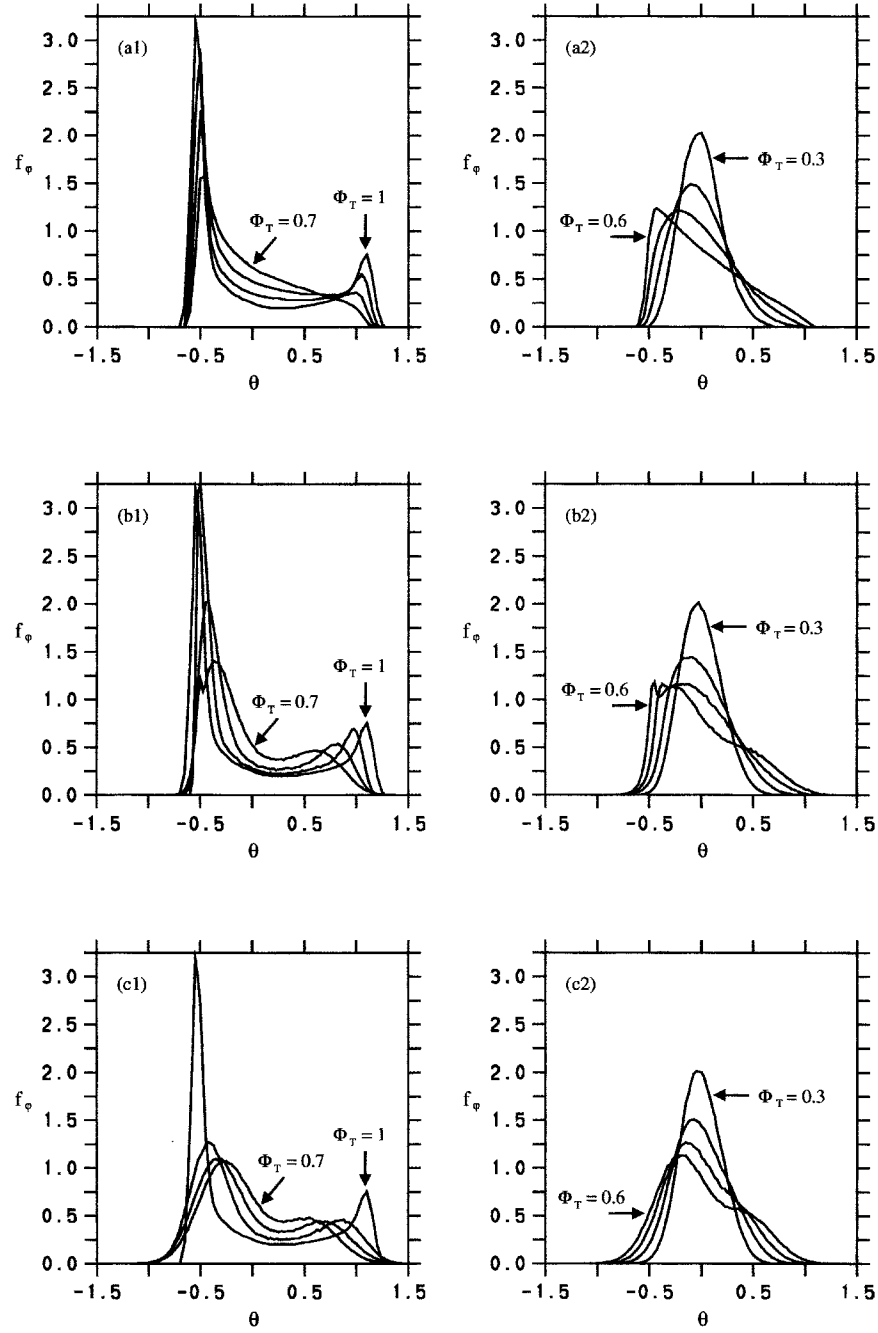
Figure 6. The same comparison as in Figure 5, but with reference to the scalar-2 PDF.

model (6.10) in the early stage of mixing ($0.7 \leq \Phi_T \leq 1$). For $\Phi_T \leq 0.6$, one finds that the predictions of both models are very similar, in particular for the scalar-1 case. This shows that memory effects are of minor relevance in this stage of mixing.

Figure 7 reveals that the joint scalar PDF predicted by the RIEM model also satisfies the boundedness constraint: the convex region in sample space occupied by the scalars decreases with time [40]. This simulation could not be performed by using the same initial condition as considered in the DNS by Juneja and Pope [25] because the model input data required for that (the initial assignment between the scalar-1 and scalar-2 values) cannot be generated sufficiently accurate. Therefore, it was assumed that there is no assignment between the values of scalar 1 and 2. This case enables the study of the transition of a rectangular initial joint PDF to the circular asymptotic joint PDF, which is very similar to the consideration of the transition from a triangular to a circular joint PDF investigated by Juneja and Pope [25]. Within the first stage of mixing ($0.7 \leq \Phi_T \leq 1$), the form of the rectangular joint PDF is preserved. After a transitional stage ($0.3 \leq \Phi_T \leq 0.6$), the form of the joint PDF changes to a circular joint PDF. The latter shape characterizes a joint Gaussian PDF for the case considered that both scalars have about the same variance. These features of the RIEM model agree well with those observed by DNS. The DNS data show a somewhat slower decay of the initial joint PDF structure in the transitional stage, but such small differences have to be expected.

7. Summary and Further Discussion

For reasons given in the introduction, the paper addresses the modeling of non-equilibrium flows by means of PDF methods. A summary of the concepts used to construct nonlinear stochastic equations for such flows is given in Section 7.1. The modeling of the influence of non-equilibrium effects on the simple linear mechanism of near-equilibrium processes, which is obtained by adopting these concepts, will be pointed out in Section 7.2. The application of the models developed here to non-equilibrium flow simulations will be discussed finally in Section 7.3.

7.1. Concepts for the extension of linear stochastic methods

The first concept for the derivation of nonlinear stochastic equations was presented in Section 3. It may be seen as the dynamic version of constructing an analytical PDF on the basis of the knowledge of a few low-order moments (see the explanations given in Appendix C). In analogy to this concept, one considers a finite number of moment transport equations. The corresponding determination of the model functions $\mathbf{\Gamma}$ and $\mathbf{\Omega}$ of the stochastic model (3.1a–3.1c) was explained in Section 3.3. It is worth noting that this concept is not only useful for the construction of nonlinear stochastic equations. Its application to the construction of
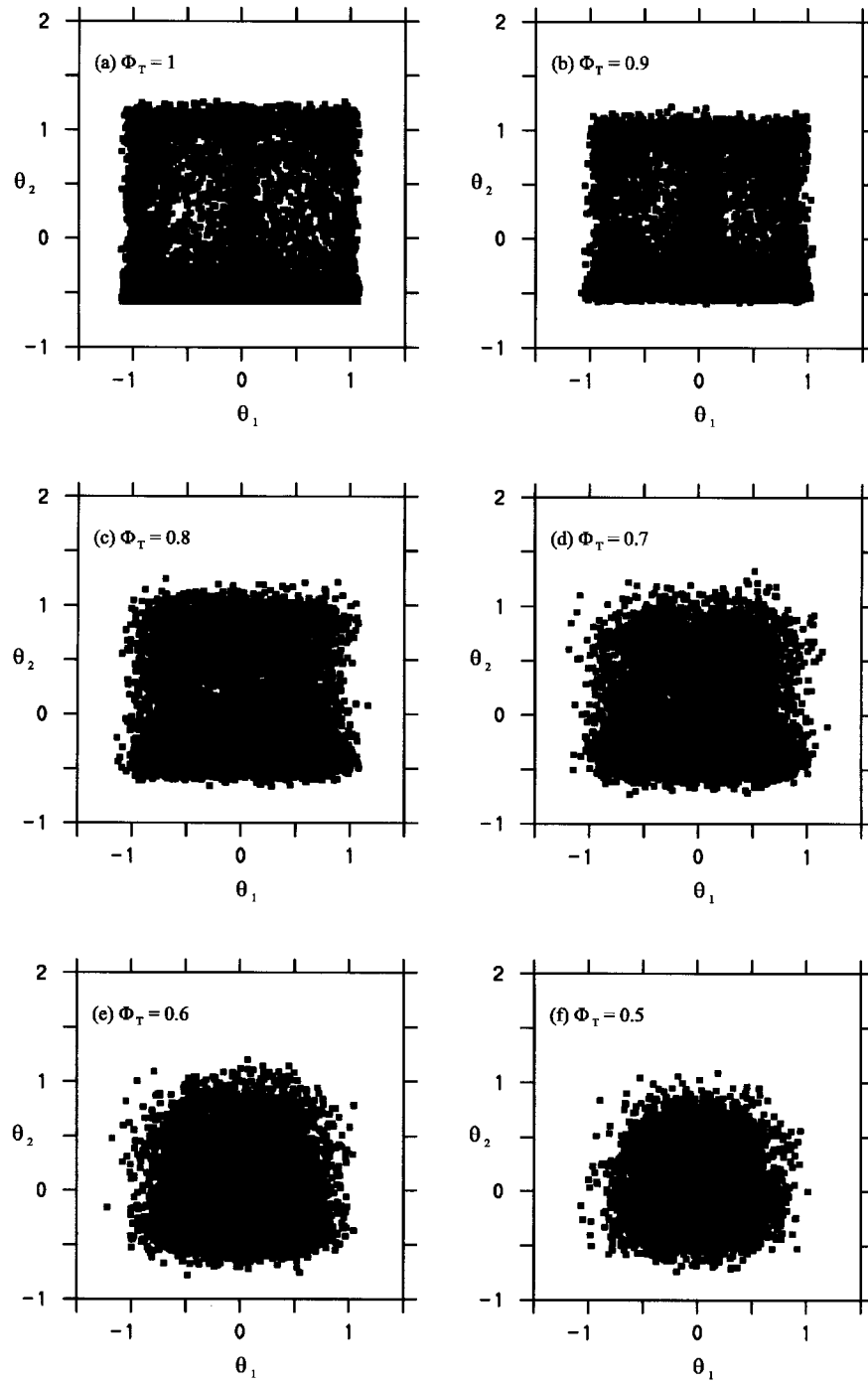
Figure 7. The evolution of the joint PDF of the scalars 1 and 2 given in a scatter plot according to the RIEM model.
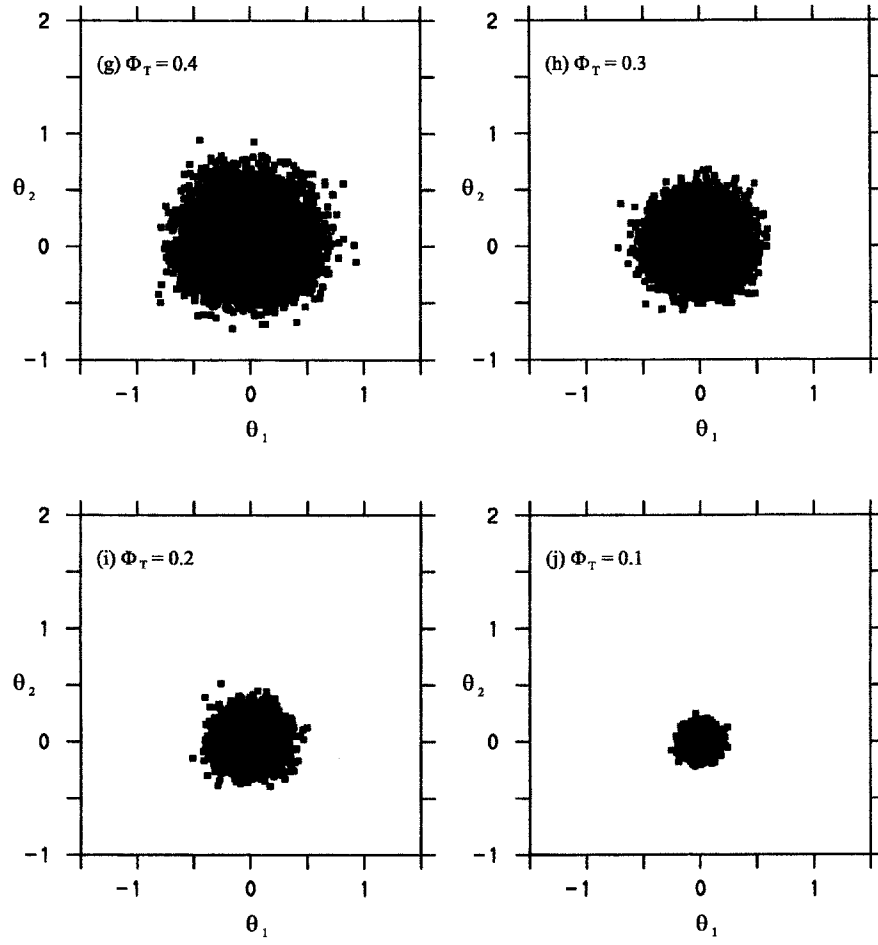
Figure 7. (Continued)

linear stochastic (and corresponding second-order RANS) methods results in new implications that are described in Section 4.3.

The second concept for the derivation of nonlinear stochastic equations was presented in Section 6. This concept makes use of the projection operator technique, which enables the extraction of the dynamics of macroscopic variables from underlying deterministic dynamics of (microscopic) quantities. Its application to the modeling of the evolution of scalar fields was presented in Sections 6.2 and 6.3. The generalized stochastic equations (6.8a–6.8b) obtained in this way involve memory effects regarding to both the stochastic forcing and relaxation of fluctuations. The relevance of involving such effects was pointed out in Section 6.1.

7.2. THE MODELING OF NON-EQUILIBRIUM EFFECTS

Stochastic methods used previously for the construction of nonlinear PDF models for non-equilibrium flows (see the references given in the introduction) require knowledge about the result of the PDF evolution (the limiting PDF) for their application. In contrast to this, the concepts described in Section 7.1 allow to describe the influence of non-equilibrium effects on the mechanism of near-equilibrium fluctuations. The following features of non-equilibrium effects are found in this way.

The basic mechanism of near-equilibrium fluctuations is their generation through delta-correlated stochastic forces and relaxation (given by a term that is linear in velocities or scalars). Both the stochastic noise generation and the mixing frequency (the negative coefficient of the velocity term in (4.1a)) are independent of the actual state of velocities and scalars. This assumption of a state-independence of the noise generation and mixing frequency becomes (in general) an invalid concept for non-equilibrium flow simulations. The requirement to involve a state-dependence of the noise production in scalar equations was pointed out in Sections 6.1 and 6.4. The need to involve a state-dependence of the mixing frequency was discussed in Sections 5.1 and 5.4. It is worth emphasizing that the consideration of a mixing frequency that depends on the actual velocity is different from the calculation of fluctuating frequencies via stochastic equations, where a velocity dependence does not appear [40].

7.3. APPLICATIONS TO NON-EQUILIBRIUM FLOW SIMULATIONS

The cubic stochastic and RIEM model developed here were applied to two flows that may be seen as cornerstones for the calculation of non-equilibrium flows of practical relevance: a convective boundary layer and binary mixing, which is characteristic for non-premixed combustion problems. The challenge related to the simulation of these flows arises from the need to reflect the appearance of large-scale structures in the convective boundary layer and strong nonlinearities in the evolution of scalar fields.

Evidence for the predictions of the cubic stochastic model was provided in Section 5.4 through comparison with measurements. Its advantage in comparison to existing methods was pointed out in Section 5.3. Evidence for the advantage of its use was provided in Section 5.4 by the comparison of its performance with that of a fourth-order SML-PDF model (see the explanations given in Appendix C).

Evidence for the predictions of the RIEM model was provided in Section 6.5 by comparison with DNS data. Its advantage compared to the use of methods presented previously is given through the significantly better agreement with DNS data: the transition from the initial to the asymptotic PDF is calculated such that the boundedness constraint is satisfied and unphysical PDF peaks near boundaries do not appear. In contrast to this, the IEM model cannot predict the transition to a Gaussian PDF for the cases considered, and the use of Fox' [12, 13] approach

(which provides better predictions than the binomial Langevin model for turbulent mixing proposed by Valiño and Dopazo [47]) results in unphysical peaks of the PDFs near boundaries (see figure 13 in Fox [12] for an illustration). In addition to this, the RIEM model was shown to be applicable to the simulation of the evolution of asymmetric PDFs and multiple scalar mixing. The comparison of the predictions of the RIEM model with those of the asymptotic model (6.10), which neglects memory effects, revealed significant advantages of the RIEM model regarding the simulation of mixing in the first stage of mixing, see the explanations given in Section 6.5.

Applications of the RIEM model to other cases do only require available information: the initial values of the standardized bounds have to be provided. A simpler way to improve existing methods is the application of the asymptotic model (6.10). This is not more demanding than the use of the standard IEM model but provides the correct asymptotic PDF. It is worth emphasizing that the applicability of the cubic stochastic model is not restricted to a specific case: it can be used to calculate any chemical processes in the day-time atmospheric boundary layer, which is of remarkable relevance. One way to apply the cubic stochastic model to other cases is to use simple parametrizations for its coefficients in correspondence to (4.1a). Another way (applied here) is to calculate these coefficients from measurements. Nevertheless, the complexity of the models presented here (which is a requirement for their applicability to non-equilibrium flow simulations) leads to questions regarding the alternative use of FDF equations for such flows. This will be addressed in a companion paper [22].

Appendix A: Second, Third- and Fourth-Order RANS Equations

The combination of the basic equations (2.1b–2.1c) with Equations (2.5b–2.5c) for averaged velocities and scalars enables the derivation of equations for the fluctuations of turbulent velocities and scalars. These equations may be used to obtain the following variance transport equations:

$$\frac{\partial \overline{u_i u_j}}{\partial t} + \bar{U}_k \frac{\partial \overline{u_i u_j}}{\partial x_k} + \langle \rho \rangle^{-1} \frac{\partial \langle \rho \rangle \overline{u_k u_i u_j}}{\partial x_k} + \overline{u_k u_j} \frac{\partial \bar{U}_i}{\partial x_k} + \overline{u_k u_i} \frac{\partial \bar{U}_j}{\partial x_k}$$
$$= \overline{a_i u_j} + \overline{a_j u_i}, \tag{A.1a}$$

$$\frac{\partial \overline{u_i \phi_\alpha}}{\partial t} + \bar{U}_k \frac{\partial \overline{u_i \phi_\alpha}}{\partial x_k} + \langle \rho \rangle^{-1} \frac{\partial \langle \rho \rangle \overline{u_k u_i \phi_\alpha}}{\partial x_k} + \overline{u_i u_k} \frac{\partial \bar{\Phi}_\alpha}{\partial x_k} + \overline{u_k \phi_\alpha} \frac{\partial \bar{U}_i}{\partial x_k}$$
$$= \overline{a_i \phi_\alpha} + \overline{a_\alpha u_i}, \tag{A.1b}$$

$$\frac{\partial \overline{\phi_\alpha \phi_\beta}}{\partial t} + \bar{U}_k \frac{\partial \overline{\phi_\alpha \phi_\beta}}{\partial x_k} + \langle \rho \rangle^{-1} \frac{\partial \langle \rho \rangle \overline{u_k \phi_\alpha \phi_\beta}}{\partial x_k} + \overline{u_k \phi_\beta} \frac{\partial \bar{\Phi}_\alpha}{\partial x_k} + \overline{u_k \phi_\alpha} \frac{\partial \bar{\Phi}_\beta}{\partial x_k}$$
$$= \overline{a_\alpha \phi_\beta} + \overline{a_\beta \phi_\alpha}. \tag{A.1c}$$

A model that applies Equations (A.1a–A.1c) to obtain the Reynolds stresses and heat fluxes in the equations for averaged variables is called a second-order RANS model. Correspondingly, third-order moment transport equations can be obtained. These equations read for the velocity field

$$
\frac{\partial \overline{u_i u_j u_k}}{\partial t} + \bar{U}_m \frac{\partial \overline{u_i u_j u_k}}{\partial x_m} + \langle\rho\rangle^{-1} \frac{\partial \langle\rho\rangle \overline{u_m u_i u_j u_k}}{\partial x_m}
$$

$$
+ \frac{\partial \bar{U}_i}{\partial x_m} \overline{u_m u_j u_k} + \frac{\partial \bar{U}_j}{\partial x_m} \overline{u_m u_i u_k} + \frac{\partial \bar{U}_k}{\partial x_m} \overline{u_m u_i u_j}
$$

$$
- \langle\rho\rangle^{-1} \left(\frac{\partial \langle\rho\rangle \overline{u_i u_m}}{\partial x_m} \overline{u_j u_k} + \frac{\partial \langle\rho\rangle \overline{u_j u_m}}{\partial x_m} \overline{u_i u_k} + \frac{\partial \langle\rho\rangle \overline{u_k u_m}}{\partial x_m} \overline{u_i u_j} \right)
$$

$$
= \overline{a_i u_j u_k} + \overline{a_j u_i u_k} + \overline{a_k u_i u_j}. \tag{A.2}
$$

A RANS model that applies (A.1a) and (A.2) to calculate $\overline{u_i u_j}$ is called a third-order RANS model. The fourth-order moment transport equations are found analogously,

$$
\frac{\partial \overline{u_i u_j u_k u_l}}{\partial t} + \bar{U}_m \frac{\partial \overline{u_i u_j u_k u_l}}{\partial x_m} + \langle\rho\rangle^{-1} \frac{\partial \langle\rho\rangle \overline{u_m u_i u_j u_k u_l}}{\partial x_m} + \frac{\partial \bar{U}_i}{\partial x_m} \overline{u_m u_j u_k u_l}
$$

$$
+ \frac{\partial \bar{U}_j}{\partial x_m} \overline{u_m u_i u_k u_l} + \frac{\partial \bar{U}_k}{\partial x_m} \overline{u_m u_i u_j u_l} + \frac{\partial \bar{U}_l}{\partial x_m} \overline{u_m u_i u_j u_k}
$$

$$
- \langle\rho\rangle^{-1} \left(\frac{\partial \langle\rho\rangle \overline{u_i u_m}}{\partial x_m} \overline{u_j u_k u_l} + \frac{\partial \langle\rho\rangle \overline{u_j u_m}}{\partial x_m} \overline{u_i u_k u_l} \right.
$$

$$
\left. + \frac{\partial \langle\rho\rangle \overline{u_k u_m}}{\partial x_m} \overline{u_i u_j u_l} + \frac{\partial \langle\rho\rangle \overline{u_l u_m}}{\partial x_m} \overline{u_i u_j u_k} \right)
$$

$$
= \overline{a_i u_j u_k u_l} + \overline{a_j u_i u_k u_l} + \overline{a_k u_i u_j u_l} + \overline{a_l u_i u_j u_k}. \tag{A.3}
$$

The common use of (A.1a), (A.2) and (A.3) to calculate $\overline{u_i u_j}$ is called a fourth-order RANS model. Equations (A.2) and (A.3) can also be applied to coupled velocity-scalar fields if the components u_k are replaced by ϕ_α, a_k by a_α and $\bar{U}_k$ by $\bar{\Phi}_\alpha$.

Appendix B: The Fokker–Planck Model for the Conditional Accelerations

One can easily prove that the condition for the consistency of the PDF transport equation (2.8) with the corresponding equation implied by the stochastic model (3.1a–3.1c) is given by

$$
0 = \frac{\partial F h_i}{\partial v_i} + \frac{\partial F h_\alpha}{\partial \theta_\alpha}, \tag{B.1}
$$

where we introduced the abbreviations

$$h_i = \Gamma_i + F_i - \frac{1}{2F}\frac{\partial b_{ij}^2 F}{\partial v_j} - \overline{A_i \mid \mathbf{v}, \boldsymbol{\theta}},$$

$$h_\alpha = \Omega_\alpha + S_\alpha - \frac{1}{2F}\frac{\partial c_{\alpha\beta}^2 F}{\partial \theta_\beta} - \overline{A_\alpha \mid \mathbf{v}, \boldsymbol{\theta}}. \tag{B.2}$$

To assess the relevance of h_i and h_α, we multiply (B.2) with any function Q of velocities and scalars, which leads (after applying partial integration) to

$$0 = \overline{\frac{\partial Q(\mathbf{U}, \boldsymbol{\Phi})}{\partial U_i} h_i} + \overline{\frac{\partial Q(\mathbf{U}, \boldsymbol{\Phi})}{\partial \Phi_\alpha} h_\alpha}. \tag{B.3}$$

The components h_i and h_α could be combined to a joint vector $\mathbf{h} = (h_i, h_\alpha)$, and, correspondingly, the velocities and scalars to a joint process. The use of suitable choices for Q reveals then that the means of h_i and h_α are zero, and that h_i and h_α are uncorrelated with any functions of velocities and scalars. Thus, h_i and h_α can be neglected such that the relations (B.2) reduce to

$$\overline{A_i \mid \mathbf{v}, \boldsymbol{\theta}} = \Gamma_i + F_i - \frac{1}{2F}\frac{\partial b_{ij}^2 F}{\partial v_j}, \quad \overline{A_\alpha \mid \mathbf{v}, \boldsymbol{\theta}} = \Omega_\alpha + S_\alpha - \frac{1}{2F}\frac{\partial c_{\alpha\beta}^2 F}{\partial \theta_\beta}. \tag{B.4}$$

The application of these expressions in (2.8) provides the Fokker–Planck equation that is implied by the stochastic model (3.1a–3.1c).

Appendix C: SML- and ETL-PDF models

The concept of determining the coefficients of Fokker–Planck equations by means of an assumed limiting PDF will only be presented for velocities. This simplifies the representation and is sufficient for the explanations given in Section 5. Scalar fields could be involved by extending the set of stochastic variables considered. According to Equation (2.8) combined with the relations (3.2), the equation for the velocity PDF $F_u(\mathbf{v}, \mathbf{x}, t) = \overline{\delta(\mathbf{U}(\mathbf{x}, t) - \mathbf{v})}$ reads

$$\frac{\partial}{\partial t}\langle\rho\rangle F_u + \frac{\partial}{\partial x_i}\langle\rho\rangle v_i F_u = -\frac{\partial}{\partial v_i}\langle\rho\rangle[\Gamma_i + F_i]F_u + \frac{1}{2}\frac{\partial^2}{\partial v_i \partial v_j}\langle\rho\rangle b_{ij}^2 F_u. \tag{C.1}$$

Thomson [45] proposed the specification of a solution to that equation in order to calculate $\boldsymbol{\Gamma}$. The PDF transport equation obtained in this way assures a PDF evolution towards that limiting solution provided that singularities do not arise from this assumed solution and the applied boundary conditions [41]. To calculate $\boldsymbol{\Gamma}$ we rewrite (C.1) as

$$\Gamma_i = \frac{1}{2F_u}\frac{\partial b_{ij}^2 F_u}{\partial v_j} + \frac{\varphi_i}{F_u} - F_i, \tag{C.2}$$

where φ_i satisfies the equation

$$\frac{\partial \langle \rho \rangle \varphi_i}{\partial v_i} = -\frac{\partial}{\partial t} \langle \rho \rangle F_u - \frac{\partial}{\partial x_i} \langle \rho \rangle v_i F_u \tag{C.3}$$

in conjunction with the boundary condition $\boldsymbol{\varphi} \to 0$ if $|\mathbf{v}| \to \infty$ [45]. The comparison of (C.2) with (3.2) reveals the relationship between φ_i and the conditional acceleration,

$$\varphi_i = \overline{A_i \mid \mathbf{v}} \, F_u. \tag{C.4}$$

A model that calculates $\boldsymbol{\Gamma}$ from an assumed limiting PDF via (C.2) will be referred to as 'evolution-towards-a-limiting' (ETL-) PDF model.

From the viewpoint of the probability theory, the most convenient way to obtain the limiting (or any other analytical) PDF based on a minimum of information (the knowledge of a few moments of low-order) is the construction of the statistically most-likely (SML-) PDF [36]. In dependence on the available moments, there exists a hierarchy of SML-PDFs. The assumption of a Gaussian PDF corresponds to a second-order SML-PDF due to the assumed availability of the first two moments. The calculation of $\boldsymbol{\Gamma}$ for this case may be found in [18]. However, a Gaussian limiting PDF has to be considered as an invalid model for many non-equilibrium flows where one finds PDFs as superposition of different modes which characterize various coherent motions [34]. To reflect such coherent structures, one has to look at a SML-PDF of higher than second-order. In the next better order of approximation, this requires the consideration of a fourth-order SML-PDF,

$$\begin{aligned}
F_u &= \frac{1}{N_F} \exp \left\{ \alpha_k (v_k - \bar{U}_k) + \frac{1}{2} \alpha_{kl} (v_k - \bar{U}_k)(v_l - \bar{U}_l) \right. \\
&\quad + \frac{1}{3} \alpha_{klm} (v_k - \bar{U}_k)(v_l - \bar{U}_l)(v_m - \bar{U}_m) \\
&\quad + \left. \frac{1}{4} \alpha_{klmn} (v_k - \bar{U}_k)(v_l - \bar{U}_l)(v_m - \bar{U}_m)(v_n - \bar{U}_n) \right\},
\end{aligned} \tag{C.5}$$

because a third-order SML-PDF (given by neglecting the last term in the exponential of (C.5)) diverges for infinitely high positive or negative values of fluctuations in sample space. In (C.5), α_k, α_{kl}, α_{klm}, α_{klmn} and N_F are parameters which are uniquely determined through the knowledge of the first four moments and the normalization condition for F_u to integrate to unity. The use of (C.5) in combination with (C.2) and (C.3) to provide $\boldsymbol{\Gamma}$ in (C.1) corresponds to a fourth-order ETL-PDF model.

A relatively simple method to calculate α_k, α_{kl}, α_{klm}, α_{klmn} in terms of the first four moments consists is the following one. By differentiation of F_u, (C.5) may be brought into the form of a Fokker–Planck equation. The multiplication with the corresponding variables and integration leads to four relations,

$$0 = \alpha_m + \alpha_{mjk} V_{jk} + \alpha_{mjkl} \overline{u_j u_k u_l}, \tag{C.6a}$$

$$0 = \alpha_{ik} V_{kj} + \alpha_{ikl}\overline{u_k u_l u_j} + \alpha_{iklm}\overline{u_k u_l u_m u_j} + \delta_{ij}, \tag{C.6b}$$

$$\begin{aligned}
0 = {} & \alpha_{ik}\overline{u_k u_j u_n} + \alpha_{ikl}[\overline{u_k u_l u_j u_n} - V_{kl} V_{jn}] \\
& + \alpha_{iklm}[\overline{u_k u_l u_m u_j u_n} - \overline{u_k u_l u_m}\, V_{jn}],
\end{aligned} \tag{C.6c}$$

$$\begin{aligned}
0 = {} & \alpha_{ik}\overline{u_k u_j u_n u_{n'}} + \alpha_{ikl}[\overline{u_k u_l u_j u_n u_{n'}} - V_{kl}\overline{u_j u_n u_{n'}}] \\
& + \alpha_{iklm}[\overline{u_k u_l u_m u_j u_n u_{n'}} - \overline{u_k u_l u_m}\,\overline{u_j u_n u_{n'}}] \\
& + \delta_{ij} V_{nn'} + \delta_{in} V_{jn'} + \delta_{in'} V_{jn}.
\end{aligned} \tag{C.6d}$$

The relations (C.6a–C.6d) are equations for α_k, α_{kl}, α_{klm}, α_{klmn}, where the fifth- and sixth-order moments appear as tensor functions of these coefficients according to (C.5). These fifth- and sixth-order moments may be found by successive approximation: (i) appropriate initial values are chosen for them, (ii) α_k, α_{kl}, α_{klm}, α_{klmn} are calculated by Equations (C.6a–C.6d), and (iii) the third- up to the sixth-order moments of F_u are computed by means of (C.5). By choosing the calculated fifth- and sixth-order moments as new initial values, this procedure is repeated until the third- and fourth-order moments provided by (C.5) agree with their known values.

Acknowledgements

References

1. Baldyga, J. and Bourne, J.R., *Turbulent Mixing and Chemical Reactions*. John Wiley & Sons, Chichester (1999).
2. Canuto, V.M., Turbulent convection with overshooting: Reynolds stress approach. *Astrophys. J.* **392** (1992) 218–232.
3. Canuto, V.M., Minotti, F., Ronchi, C., Ypma, R.M. and Zeman, O., Second-order closure PBL model with new third-order moments: Comparison with LES data. *J. Atmos. Sci.* **51** (1994) 1605–1618.
4. Craft, T.J., Kidger, J.W. and Launder, B.E., Importance of third-moment modeling in horizontal, stably-stratified flows. In: *Proceedings of the 11th Symposium on Turbulent Shear Flows*, Grenoble, France (1997) pp. 2013–2018.
5. Craft, T.J., Developments in a low-Reynolds number second-moment closure and its application to separating and reattaching flows. *Internat. J. Heat Fluid Flow* **19** (1998) 541–548.

6. Dopazo, C., Recent developments in PDF methods. In: Libby, P.A. and Williams, F.A. (eds.), *Turbulent Reacting Flows*. Academic Press, San Diego, CA (1994) pp. 375–474.

7. Du, S., Wilson, J.D. and Yee, E., Probability density functions for velocity in the convective boundary layer, and implied trajectory models. *Atmos. Environ.* **28** (1994) 1211–1217.

8. Du, S., Wilson, J.D. and Yee, E., On the moments approximation method for constructing a Lagrangian stochastic model. *Bound.-Layer Meteorol.* **40** (1994) 273–292.

9. Du, S., Sawford, B.L., Wilson, J.D. and Wilson, D.J., Estimation of the Kolmogorov constant (C_0) for the Lagrangian structure function, using a second-order Lagrangian model of grid turbulence. *Phys. Fluids* **7** (1995) 3083–3090.

10. Durbin, P.A. and Speziale, C.G., Realizability of second-moment closure via stochastic analysis. *J. Fluid Mech.* **280** (1994) 395–407.

11. Eswaran, V. and Pope, S.B., Direct numerical simulations of the turbulent mixing of a passive scalar. *Phys. Fluids* **31** (1988) 506–520.

12. Fox, R.O., The Fokker–Planck closure for turbulent molecular mixing: Passive scalars. *Phys. Fluids A* **4** (1992) 1230–1244.

13. Fox, R.O., Improved Fokker–Planck model for the joint scalar, scalar gradient PDF. *Phys. Fluids* **6** (1994) 334–348.

14. Fox, R.O., Computational methods for turbulent reacting flows in the chemical process industry. *Rev. Inst. Français du Pétrole* **51** (1996) 215–243.

15. Fox, R.O., On velocity-conditioned scalar mixing in homogeneous turbulence. *Phys. Fluids* **8** (1996) 2678–2691.

16. Gardiner, C.W., *Handbook of Statistical Methods*. Springer-Verlag, Berlin (1983).

17. Grabert, H., *Projection Operator Technique in Nonequilibrium Statistical Mechanics*. Springer-Verlag, Berlin (1982).

18. Heinz, S., Nonlinear Lagrangian equations for turbulent motion and buoyancy in inhomogeneous flows. *Phys. Fluids* **9** (1997) 703–716.

19. Heinz, S., Time scales of stratified turbulent flows and relations between second-order closure parameters and flow numbers. *Phys. Fluids* **10** (1998) 958–973.

20. Heinz, S., Connections between Lagrangian stochastic models and the closure theory of turbulence for stratified flows. *Internat. J. Heat Fluid Flow* **19** (1998) 193–200.

21. Heinz, S. and van Dop, H., Buoyant plume rise described by a Lagrangian turbulence model. *Atmos. Environ.* **33** (1999) 2031–2043.

22. Heinz, S., On Fokker–Planck equations for turbulent reacting flows. Part 2. Filter density function for large eddy simulation. *Flow, Turb. Combust.* **70** (2003) 153–181.

23. Heinz, S., *Statistical Mechanics of Turbulent Flows*. Springer-Verlag, Berlin (2003).

24. Ilyushin, B.B. and Kurbatski, A.F., Modeling of turbulent transport in PBL with third-order moments. In: *Proceedings of the 11th Symposium on Turbulent Shear Flows*, Grenoble, France (1997) pp. 2019–2024.

25. Juneja, A. and Pope, S.B., A DNS study of turbulent mixing of two passive scalars. *Phys. Fluids* **8** (1996) 2161–2184.

26. Kassinos, S., Reynolds, W.C. and Rogers, M.M., One-point turbulence structure tensors. *J. Fluid Mech.* **428** (2001) 213–248.

27. Kawamura, H., Sasaki, J. and Kobayashi, K., Budget and modeling of triple moment velocity correlations in a turbulent channel flow based on DNS. In: *Proccedings of the 10th Symposium on Turbulent Shear Flows*, Pennsylvania State University (1995) pp. 2613–2618.

28. Kerstein, A.R., Linear-eddy modeling of turbulent transport. II: Application to shear layer mixing. *Combust. Flame* **75** (1989) 397–413.

29. Kerstein, A.R., Linear-eddy modeling of turbulent transport. Part 3. Mixing and differential molecular diffusion in round jets. *J. Fluid Mech.* **216** (1990) 411–435.

30. Kerstein, A.R., One-dimensional turbulence: Model formulation and application to homogeneous turbulence, shear flows, and buoyant stratified flows. *J. Fluid Mech.* **392** (1999) 277–334.

31. Kuo, K.K., *Principles of Combustion*. Wiley Interscience, New York (1986).

32. Launder, B.E., Phenomenological modeling: Present and future. In: Lumley, J.L. (ed.), *Wither Turbulence? Turbulence at the Crossroads*. Springer-Verlag, Berlin (1990) pp. 439–485.

33. Lindenberg, K. and West, J.W., *The Nonequilibrium Statistical Mechanics of Open and Closed Systems*. VHC Publishers, New York (1990).

34. Luhar, A.K., Hibberd, M.F. and Hurley, P.J., Comparison of closure schemes used to specify the velocity PDF in Lagrangian stochastic dispersion models for convective conditions. *Atmos. Environ.* **30** (1996) 1407–1418.

35. Peters, N., *Turbulent Combustion*. Cambridge University Press, Cambridge (2001).

36. Pope, S.B., Probability distributions of scalars in turbulent shear flow. In: Bradbury, L.S.S., Durst, F., Launder, B.E., Schmidt, F.W. and Whitelaw, J.H. (eds.), *Turbulent Shear Flows 2*. Springer-Verlag, Berlin (1980) pp. 7–16.

37. Pope, S.B., PDF methods for turbulent reactive flows. *Prog. Energy Combust. Sci.* **11** (1985) 119–192.

38. Pope, S.B., On the relationship between stochastic Lagrangian models of turbulence and second-moment closures. *Phys. Fluids* **6** (1994) 973–985.

39. Pope, S.B., The vanishing effect of molecular diffusivity on turbulent dispersion: Implications for turbulent mixing and the scalar flux. *J. Fluid Mech.* **359** (1998) 299–312.

40. Pope, S.B., *Turbulent Flows*. Cambridge University Press, Cambridge (2000).

41. Risken, H., *The Fokker–Planck Equation*. Springer-Verlag, Berlin (1984).

42. Sawford, B.L., Recent developments in the Lagrangian stochastic theory of turbulent dispersion. *Bound.-Layer Meteorol.* **62** (1993) 197–215.

43. Sawford, B.L., Rotation of Lagrangian stochastic models of turbulent dispersion. *Bound.-Layer Meteorol.* **93** (1999) 411–424.

44. Speziale, C.G. and Xu, X., Towards the development of second-order closure models for nonequilibrium turbulent flows. *Internat. J. Heat Fluid Flow* **17** (1996) 238–244.

45. Thomson, D.J., Criteria for the selection of stochastic models of particle trajectories in turbulent flows. *J. Fluid Mech.* **180** (1987) 529–556.

46. Thomson, D.J. and Montgomery, M.R., Reflection boundary conditions for random walk models of dispersion in non-Gaussian turbulence. *Atmos. Environ.* **28** (1994) 1981–1987.

47. Valiño, L. and Dopazo, C., A binomial Langevin model for turbulent mixing. *Phys. Fluids A* **3** (1991) 3034–3037.

48. Van Dop, H., Nieuwstadt, F.T.M. and Hunt, J.C.R., Random walk models for particle displacements in inhomogeneous unsteady turbulent flows. *Phys. Fluids* **28** (1985) 1639–1653.

49. Wilson, J.D. and Sawford, B.L., Review of Lagrangian stochastic models for trajectories in the turbulent atmosphere. *Bound.-Layer Meteorol.* **78** (1996) 191–210.

50. Zubarev, D., Morozov, V. and Röpke, G., *Statistical Mechanics of Nonequilibrium Processes. Vol. 1: Basic Concepts, Kinetic Theory*. Akademie Verlag (VCH Publishers), Berlin (1996).

51. Zubarev, D., Morozov, V. and Röpke, G., *Statistical Mechanics of Nonequilibrium Processes. Vol. 2: Relaxation and Hydrodynamic Processes*. Akademie Verlag (VCH Publishers), Berlin (1997).